scientific reports

Check for updates

OPEN

Effects of infrared assisted refractance window drying on physicochemical and quality attributes and thermodynamic analysis of thyme (*Thymus vulgaris* L.)

Shahin Zomorodi[1]✉, Mohammad Kaveh[2], Mahnaz Heidari Rikan[1], Szymanek Mariusz[3]✉ & Agata Dziwulska-Hunek[4]

In this research, the process of drying thyme with Infrared- assisted Refractance Window (IR-RW) method was investigated as a new technology. The effect of water temperature (WT) and weight of samples (SW) on kinetics, energy, thermodynamic properties, qualitative characteristics, bioactive and essential oil were determined and optimized. Based on the response surface method (RSM-CCD), WT (70-90 °C) and SW (60-120 g) to achieve the best drying time, energy consumption (SEC), color (ΔE), bioactive properties and essential oil efficiency (EO) were optimized. The results showed that Midilli's model evaluates the stages of drying of the thin layer of thyme more appropriately than other models. Also, the effective diffusivity (D_{eff}) and Activation Energy (Ea), enthalpy (ΔH), entropy (ΔS) and Gibbs free energy (ΔG) were obtained between 8.67×10^{-9}- 3.02×10^{-8} m^2/s, 20.71- 31.17 kJ/mol, 17.69-28.31 kJ/mol, -0.1490- -0.118 kJ/mol K and 67.69-73.04 kJ/mol, respectively. Increasing the WT raises the DR, brightness, AA, D_{eff} and ΔH and decreases the drying time, SEC, ΔH, ΔG, CO_2, Chroma, a*, b* and ΔE. The highest value of total phenol content (TPC), rehydration ratio (RR), EO was recorded at the WT of 80 °C and the SW was 90 g. The optimal values of the process variables are 85.02 °C for water temperature (WT) and 86.10 g for sample weight (SW). In addition to these values, the optimal values for drying time, SEC, ΔE, AA, TPC, TFC and OE were 91.003 minutes, 8.37 kWh/kg, 1.42, 71.68%, 37.93 mg GAE/ 100 g d.m, 35.11 mg QE/100 g d.m and 2.04%, respectively, at the desirability value of 0.807. Thus, these findings provide valuable insights for producers regarding the drying characteristics and properties of thyme.

Keywords Infrared- assisted refractance window, Energy, Total flavonoid content, Modeling, CO_2

Abbreviations

AA	Antioxidant activity (%)
A_{Sample}	Absorbance values of sample (-)
$A_{control}$	Absorbance values of the control (-)
C	Chroma (-)
D_{eff}	Effective moisture diffusivity (m^2/s)
Ea	Activation energy (J/mol)
Et	Total energy (kWh)
h_p	Planck constant (6.626×10^{-37} $m^2.kg$)

[1]Agricultural Engineering Research Department, West Azerbaijan Agricultural and Natural Resources Research and Education Center, AREEO, Urmia, Iran. [2]Department of Petroleum Engineering, College of Engineering, Knowledge University, Erbil, Iraq. [3]Department of Agricultural, Forest and Transport Machinery, University of Life Sciences in Lublin, Głeboka, 28, 20-612 Lublin, Poland. [4]Department of Biophysics, University of Life Sciences in Lublin, Akademicka 13, 20-950 Lublin, Poland. ✉email: s.zomorodi@areeo.ac.ir; mariusz.szymanek@up.lublin.pl

K_b	Boltzmann constant (1.38 x 10^{-26} J/K)
L	The thickness of the thyme (m)
M_e	Equilibrium moisture content (% d.b)
MR	Moisture ratio (-)
M_o	Final moisture content (% d.b)
M_t	Moisture content at time t (% d.b)
$MR_{exp,i}$	Experimental moisture fraction (-)
$MR_{pre,i}$	Predicted moisture fraction (-)
M(t + Δt)	moisture content at (t + Δt) moment (% d.b)
N	Number of observations (-)
R	Universal gas constant (8.314 J/mol. K)
RMSE	Root mean square error (-)
R^2	Coefficient of explanation (-)
SEC	Energy consumptio (kWh/kg)
t	Drying time(s)
T	Absolute temperature (K)
TPC	Total phenol content (mg GAE/100 g d.m)
TFC	Total flavonoid content (mg QE/g d.m)
w	Moisture removed (kg)
y_k	Dependent variable
Zr	Wight of rehydrate thyme (g)
Zd	Weight of dried thyme (g)
UNFCCC	United Nations Convention on Climate Change
ΔH	Enthalpy:J/mol (ΔH)
ΔG	Gibbs free energy (J/mol)
ΔS	Entropy (J/mol. K)
Δt	time intervals (min)
β0	Intercept (-)
βi	Linear (-)
βii	Quadratic (-)
βij	Factors interaction coefficient (-)
χ^2	chi-square (-)
ΔE	Color change (-)

Garden thyme with the scientific name *Thumus vulgaris* is a perennial plant native to the eastern Mediterranean region[1]. Thyme has dense, branched bushes and a straight root with many branches, and the height of the bushes is usually between 20 and 50 cm. Among the medicinal uses of the essential oil of this plant, we can refer to medicines to strengthen the stomach, dilate the respiratory tract and reduce cough, anti-spasm, rheumatism and sciatica, and eliminate the weak action of the digestive system[2,3]. Today, most of the developed countries in the world are suffering from side effects caused by the use of synthetic drugs, the unaffordability of manufacturing some synthetic drugs, and the exclusivity of treating certain diseases—such as leprosy and salak—using medicinal plants, leading them to increasingly turn to medicinal plants for treatment[4]. High moisture content in fruits and medicinal plants has a significant role in storing them, decreasing moisture content or drying by means of the simultaneous transfer of mass and heat largely to raise shelf life, preserve quality and decrease loss after harvesting agricultural products to produce fruits, vegetables and dried medicinal plants[5]. Drying is one of the most important post-harvest processing operations that transforms perishable and short-lived products such as the medicinal plant thyme into resistant products with a long shelf life[6]. This process is very important in the processing of medicinal plants, because if the essential medicinal plants are not dried immediately, they lose their effective substances and volatile compounds, also research has shown that the aromatic compounds of the plants are influenced by processing methods. If the plant is dried immediately after harvesting, it helps to preserve the color and aromatic substances of the plant[7,8].

In the field of development of dryers, new drying ways are suggested to better meet consumer demands for high quality and productivity product, and environmental sustainability[9]. In recent years, many countries and government organizations that are members of the UNFCCC have emphasized reducing energy consumption and greenhouse gas emissions worldwide[10]. For this reason, there is a significant need to develop new drying techniques[11]. The drying technology first started using solar energy and developed over time and is divided into four generations[12]. First generation dryers (kiln, tray, tunnel, truck tray) use hot air flow to remove moisture from the product. Second generation dryers use thermal energy to dry slurry into powder (drum and spray), while third generation dryers use non-thermal energy to dry fruit, vegetables and medicinal plants (freeze and osmotic)[11]. The fourth generation dryers (microwave, high-vacuum, radio-frequency and RW) represent the latest development in drying technologies, where it is possible to maintain better quality of the desired products[12–14]. In this regard, hybrid-drying methods are being developed in which two or more methods are combined. According to Rajoriya et al.,[15] we can divide the hybrid drying technique into combined, multi-stage and multi-process drying. In hybrid drying, infrared heating or microwaves are combined with other drying methods, which, due to the synergistic effect, leads to the production of high-quality products and lower energy consumption, especially for heat-sensitive products. There are some benefits for it compared to conventional or single-stage drying[16].

Dryers with Infrared (IR) radiation, which are more popular than other usual systems, have benefits such as decreasing drying time, preserving product quality, and raising energy efficiency[17]. In spite of surface

irregularities, IR dryers can provide consistent heating and produce eve high quality products[18]. Since IR lamps were easily connected to other dryers, various IR combined drying systems such as vacuum-IR drying[19], hot air-IR drying[20,21], heat pump-IR[22], IR-microwave[23] were developed in the last decade. The positive role of IR alone or in combination with other methods increases the bioactive properties (TPC, TFC and AA) in dry *Ginkgo biloba L.* compared to the fresh sample[24], shortens the drying time and increasing essential oil content in *Lippia citriodora* samples[25], increasing drying rate and essential oil content, reducing drying time and microbial contamination in *Dracocephalum kotschyi*[18], improving TPC, TFC and AA, reducing the drying time and SEC compared to conventional methods in drying *Chrysanthemums*[26].

RW is an innovative, emerging and non-thermal drying technique of the fourth generation for products such as puree, leather and heat-sensitive parts of fruits and vegetables, which is gaining an acceptance in the food dehydration area[12,27]. The RW drying technique consists of a heating medium (hot water below the boiling point), a water circulation system and a Mylar plate[15]. During drying, the food is evenly distributed over a Mylar plate placed over hot water, concerning the environment. The thermal energy of the heating device which flows through the tank is moved to the material which is dried by conduction and radiation, as the thermal energy from the hot water is transferred to the food through the Mylar sheet[28]. The moisture of the products placed on the Mylar sheet evaporates due to the rapid movement of the thermal energy of the water[12]. Compared to conventional dryers, RW provides higher drying rates for heat-sensitive products with lowest damage to bioactive/nutritional components, vitamin C, color, and aroma that produce products with good shelf life and better quality in a shorter period of time with less energy consumption[11,29,30]. In addition, they have energy efficiency (28 to 38 %) 13, 31 and very high thermal efficiency (55 to 72%)[12]. In terms of food waste, this drying technology is better than second generation dryers because the drying water is returned to the tank and reheated instead of being wasted in the drying process. 15 In addition, RW requires less capital (50-70%)[12] and reduces energy consumption by 50%[31].

RW technique is mainly used to produce powder/ puree/ flakes/ pulp/ leather/ paste/ fruit slice from fruits and vegetables such as carrot[32], banana[15,33,34], apple[35–37], mango[38], jamun[39], Dragon[40], sweet cherry[41], pomegranate[42,43], goldenberry[44], Onion[45], tomato[46], physalis[47], Mango and Avocado[48], pineapple[6] and beetroot[49]. However, in recent years, RW drying has also attracted considerable attention in the production of dried medicinal plants. Studies on the preparation of medicinal plants from coriander[50], *Dracocephalum kotschyi*[18], mint[51] and Aloe vera[12] have been reported. These studies showed that RW is a promising and practical drying technique due to its SEC and low processing cost to produce dried medicinal plants with high quality (better appearance) and high nutritional value (preserving vitamins and antioxidants).

Currently, the application of two or more techniques (hybrid drying) is considered for food dehydration, as it gives a synergistic effect and improves process efficiency[52]. Few studies have been reported on the combination of IR with RW for drying various food materials. Among them, the drying of banana leather[15], apple slices[52], *Dracocephalum kotschyi*[18], okra slices[53] and Malabar spinach[54] can be mentioned.

Considering the importance and sensitivity of thyme in terms of preserving its color, aromatic compounds, and bioactive properties, its drying process is very sensitive. Furthermore, the use of new methods in drying agricultural products is crucial regarding obtaining high-quality products with the highest amount of nutrients. On the other hand, a review of the literature revealed that there is a significant gap in the existing knowledge regarding the analysis of thyme drying using a IR-RW dryer. Therefore, the aim of this study is to evaluate the performance of an IR-RW dryer for drying thyme. Various parameters, such as drying kinetics, SEC, emission of pollutants (CO_2), some qualitative characteristics (color, RR, AA, TPC and TFC) and essential oil were investigated using IR-RW. Finally, the effects of experimental parameters including water temperature and different weights on drying time, SEC, some other qualitative characteristics (color changes, AA, TPC, TFC) and essential oil extraction using RSM method were investigated and were optimized.

Materials and methods

Preparation of the raw material

To carry out this research, leaves and branches of thyme (*Thymus Vulgaris*. L) plant were taken from a distance of 4 to 5 cm from the ground and from the experimental farm of medicinal plants of West Azerbaijan Agricultural Research Center (Permission to harvest, identify, and collect them was obtained from Prof. Shahin Zomordi and Mahnaz Heidari Rikan for this study). Control specimens are available in a public herbarium at this research center. In order to prevent removal of surface moisture and wilting, fresh thyme leaves were packed in polyethylene plastic bags. Then it was kept in the refrigerator until the beginning of the experiments. To use them for drying, the initial moisture content (MC) was recorded about 82.6% (w.b) in three replicates (according to AOAC standards)[55].

Infrared- assisted refractance window dryer

Figure 1 shows the main components of an IR-RW dryer. The IR-RW dryer consists of a stainless steel frame, funnel, Mylar plate with a thickness area of 0.26 mm and 50 × 200 cm^2, respectively, as a plastic membrane, two centrifugal hot water pump (to circulate hot water), 100 liter static thermal water tank made of steel, heating unit (electric heater), fan and thermometer. Mylar plate was placed on top of the shallow hot water tank. Electric fans were placed at the top and bottom of the funnel to remove moisture during the drying process. An infrared lamp (NIR, Noor Lamp Co.) was installed on top of the Mylar plate to increase the heat and temperature. Utilizing hot water exactly below boiling temperature, the thin Mylar sheet and the infrared power all work together to enable rapid drying. All the parts of the IR- RW dryer were placed on a steel skeleton. The electronic water temperature control equipment, centrifugal hot water pump control, infrared lamp control and ventilators were installed in a control panel. Thyme with moisture content (82.6± 0.2 % (w.b)) was uniformly and thinly spread on the surface of the Mylar film, which would obtain thermal energy through the hot water surface and causes

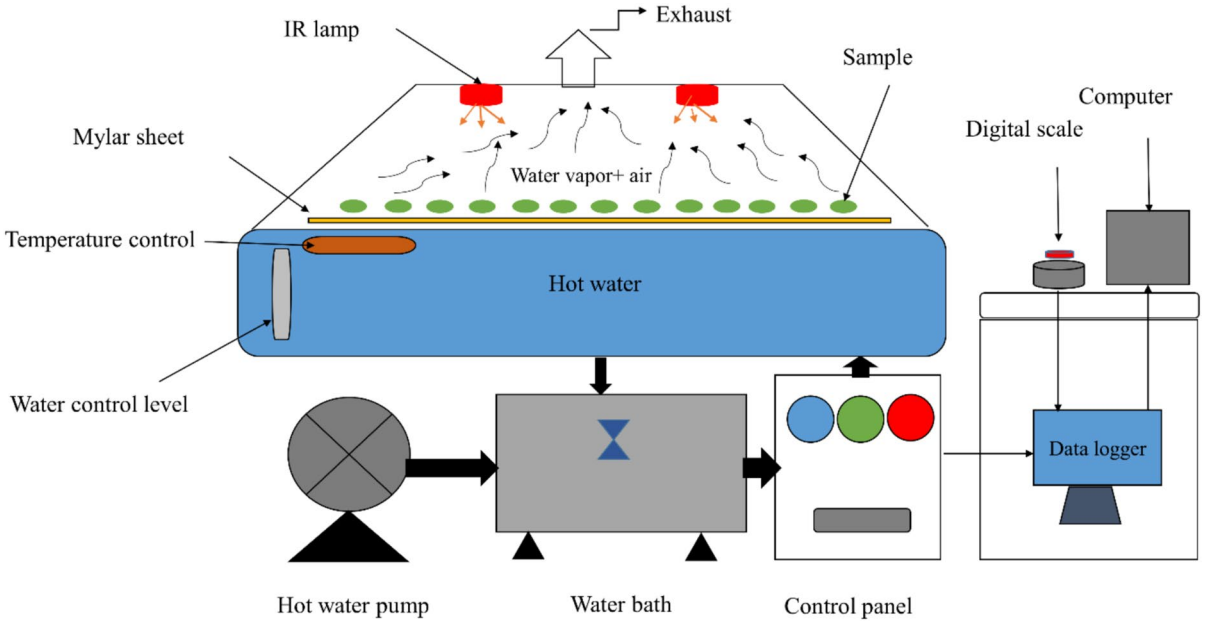

Fig. 1. Schematic diagram of the experimental setup of infrared- refractance window

sample to dry rapidly. The IR-RW drying method was set with water temperature of 70, 80 and 90 ± 0.5 °C based on preliminary tests.

Drying kinetics

The most common models of drying curves, which are used in most researches to fit laboratory data, are obtained by plotting the changes in the moisture ratio (MR) in terms of drying time. The moisture ratio is calculated according to Eq. 1:[49,56]

$$MR = \frac{M_t - M_e}{M_o - M_e} \tag{1}$$

According to previous studies and due to the long drying time of thyme, M_e values are very small compared to M_0 and M_t values. Therefore, equilibrium MC was not considered in this article and Eq. (1) was simplified as Eq. (2)

$$MR = \frac{M_t}{M_o} \tag{2}$$

Eq. 3 was used to determine the drying rate of thyme[57,58].

$$DR = \frac{M_{(t+\Delta t)} - M_t}{\Delta t} \tag{3}$$

Modeling

The experimental models of thin layer drying of foods shown in Table 1 were used to model the obtained data (MR changes against drying time). By using the R^2, RMSE and χ^2 equations, the efficiency of the mentioned modeling methods were determined and compared. It should be mentioned that higher R^2 and RMSE and lower χ^2 shows the high efficiency of the model. These equations are expressed in relations 4, 5 and 6 [50,59].

$$R^2 = 1 - \frac{\sum_{i=1}^{N} [MR_{pre,i} - MR_{real,i}]^2}{\sum_{k=1}^{N} [MR_{pre,mean} - MR_{real,i}]^2} \tag{4}$$

$$RMSE = \left[\frac{1}{N}\sum_{i=1}^{N} (MR_{pre,i} - MR_{real,i})^2\right]^{\frac{1}{2}} \tag{5}$$

Model name	Model formula	Reference
Page	$MR = \exp(-kt^n)$	Uribe et al.,[47]
Wang and Singh	$MR = 1 + at + bt^2$	Mandale et al.,[49]
Newton/Lewis	$MR = \exp(-kt)$	Nguyen et al.,[48]
Verma et al	$MR = a\exp(-kt) + (1-a)\exp(-gt)$	Venkateshwari et al.,[5]
Logarithmic	$MR = a\exp(-kt) + c$	Zalpouri et al.,[50]
Henderson and Pabis	$MR = a\exp(-kt)$	Muyonga et al[6]
Midilli et al.,	$MR = a\exp(-kt^n) + bt$	Öztekin et al.,[60]
Two-term	$MR = a\exp(-kt) + c\exp(-k_0 t)$	Simsek and Süfer,[41]

Table 1. Mathematical models applied to the drying curves

$$\chi^2 = \frac{\sum_{i=1}^{N} (MR_{real,i} - MR_{pre,i})^2}{N - z} \tag{6}$$

D_{eff}, Ea and thermodynamic parameters

Fick's law describes moisture transfer in the descending stage of the drying process (Eq. 7)[61,62]

$$\frac{\partial x}{\partial t} = D_{eff}\frac{\partial^2 x}{\partial x^2} \tag{7}$$

Studying the propagation of Fick's second law indicates mass penetration during the period of decreasing drying speed of agricultural products. Fick's Eq. is solved for different geometrical shapes by using appropriate initial and boundary conditions. For a thin blade, the solution of the Fick's Eq. is obtained from Eq. (8) [49,63]:

$$MR = \frac{M_t - M_e}{M_b - M_e} = \frac{8}{\pi^2}\sum\nolimits_{n=1}^{\infty}\frac{1}{(2n+1)}\exp\left(\frac{-D_{eff}(2n+1)^2\pi^2 t}{4L^2}\right) \tag{8}$$

The D_{eff} is obtained from the slope of the Eq. (9) line[64].

$$\ln(MR) = \ln(\frac{8}{\pi^2}) - \ln\left(\frac{\pi^2}{4L^2}D_{eff}.t\right) \tag{9}$$

The D_{eff} is usually determined by plotting the drying laboratory data in terms of ln(MR) against time. The slope of the obtained line is put in Eq. (10) to calculate the penetration coefficient[45]:

$$K_1 = \left(\frac{D_{eff}\pi^2}{4L^2}\right) \tag{10}$$

K_1 is the slope of the line.

The E_a was calculated using Eq. (11) [61]:

$$D_{eff} = D_o\exp\left(\frac{E_a}{RT}\right) \tag{11}$$

To calculate E_a, Eq. (10) can be written as Eq. (12) [52]:

$$\ln(D_{eff}) = \ln(D_o) - \left(\frac{E_a}{R}\right)\left(\frac{1}{T}\right) \tag{12}$$

Finally, the Ea can be calculated using the following Eq. (13) [2]:

$$K_2 = \left(\frac{E_a}{R}\right) \tag{13}$$

Understanding the thermodynamic properties of agricultural products is very important for designing drying equipment, investigating the characteristics of absorbed water, evaluating the microstructure of food (chemical and biochemical phenomena of β-carotene decomposition) and physical events on its surface[65,66]. Based on the obtained E_a values and the global gas constant (R), the values of enthalpy (ΔH), entropy (ΔS) and Gibbs free energy (ΔG) are calculated using Eqs. 14-16, respectively[52,61].

$$\Delta \mathrm{H} = E_a - RT \tag{14}$$

$$\Delta S = R\left[\ln(D_0) - \ln\left(\frac{K_b}{h_p}\right) - \ln(T)\right] \tag{15}$$

$$\Delta G = \Delta \mathrm{H} - T\Delta S \tag{16}$$

Specific energy consumption and CO_2 emissions

A digital energy meter (BENETECH GM86, China) was used to record the electrical energy during the thyme drying process and the SEC was calculated using Eq. (17) as mentioned by Rajoriya et al.,[15].

$$SEC(kWh/kg) = \frac{\mathrm{E_t}}{\mathrm{w}} \tag{17}$$

CO_2 emissions were measured based on the method mentioned in the study of Motevali and Koloor[67], and Kaveh et al.,[68]. In order to obtain 1 kWh of energy, the type of fuel (Natural gas (NG), Heavy Oil (HO) or Gas oil (GO)) was used in different electricity power plants in Iran (Steam (SP), Gas-turbine (GT) and Combine-cycle (CC))

Color

In most food industry research, CIE L*a*b color space is used to analyze the color change in the drying process[69]. FRU WR10-Chroma Meter-China device was used to measure the color before and after drying thyme. After measuring the color, Eqs. (18) and (19) was used to calculate the overall color changes (ΔE) and Chroma during the thyme drying process[70,71].

$$\Delta E = \sqrt{(L^* - L_O^*)^2 + (a^* - a_0^*)^2 + (b^* - b_0^*)^2} \tag{18}$$

$$C = \sqrt{(a^*)^2 + (b^*)^2} \tag{19}$$

The Browning Index (BI) was calculated from CIE L* a* b* according to Eq (20, 21)

$$BI = \frac{100(x - 0.31)}{0.172} \tag{20}$$

$$x = \frac{a^* + 1.75L^*}{5.645L^* + a^* - 3.012b^*} \tag{21}$$

Rehydration ratio

In order to measure RR, dried thyme samples (2 g) were placed in distilled water (approximately 25 °C) in time intervals of 30 to 150 minutes. Then their surface water was removed using filter paper[72]. Finally, after the weight of the samples remained constant over time, the RR was calculated using Eq. (22) [73].

$$RR = \frac{\mathrm{Z_r}}{\mathrm{Z_d}} \tag{22}$$

Antioxidant activity

AA of thyme samples was measured by the free radical neutralization (DPPH) (2,2,-diphenyl-2-picrylhydrazyl) proposed by Zalpour et al.,[50] with a slight modification. For this purpose, the samples were first diluted in the ratio of 1:18. Then 25 µL of the sample was mixed with 100 µL of DPPH. Its absorbance was read at a wavelength of 515 nm using a spectrophotometer. AA percentage was calculated by Eq. 23 [37].

$$AA(\%) = \left(1 - \frac{A_{sample}}{A_{control}}\right) \times 100 \tag{23}$$

Total Phenol

The TPC was determined based on the colorimetric method and using Folin-Ciocalteu (FC) reagent according to the method provided by Zhang et al.,[39] with some changes. Therefore, the amount of 0.5 ml of the extract prepared from the powder was mixed with 5 ml of FC reagent (10 times diluted with water) and was kept in a stationary state for 3-6 minutes. Next, 4 ml of 7.5% sodium carbonate was added to it and mixed. The light absorption of the solutions was read after 60 minutes in the dark at a wavelength of 765 nm

TFC

50 µL of the extract was combined with 1 mL of distilled water and according to the method of Zamani et al.,[18] The next step was adding 0.075 mL of sodium nitrite (5%) to it and after 5 minutes, we added 0.15 mL AlCl3 solution (10%) and after 6 minutes, 0.50 mL of NaOH (1 M) was added to the rest. The ultimate volume of the solution became 3 mL by distilled water and the intensity of the pink color appeared in the solution at the wavelength of 510 nm was recorded by spectrophotometer.

Name	Goal	Lower limit	Upper limit	Lower weight	Upper weight	Importance
A: Temperature	Is in range	70	90	1	1	3
B: Weight	Is in range	60	120	1	1	3
Time (min)	Minimize	60	230	1	1	3
SEC (kWh/kg)	Minimize	5.25	16.63	1	1	3
ΔE	Minimize	0.86	7.26	1	1	3
AA (%)	Maximize	45.48	75.73	1	1	3
TPC (mg GAE/ 100 g d.m)	Maximize	24.15	40.56	1	1	3
TFC (mg QE/100 g d.m)	Maximize	21.15	37.07	1	1	3
EO (%)	Maximize	1.49	2.35	1	1	3

Table 2. Independent variable values, the weights and importance of the parameters for infrared- refractance window dried thyme

	Independent variables		Response						
Run	Weight (g)	Water temperature (°C)	Time (min)	SEC (kWh/kg)	ΔE	AA (%)	TPC (mg GAE/ 100 g d.m)	TFC (mg QE/100 g d.m)	EO (%)
1	60	70	150	9.58	6.52	45.48	24.15	21.15	1.78
2	120	70	230	16.63	7.26	49.09	26.55	24.94	1.74
3	90	80	115	10.08	2.13	67.39	38.46	35.47	2.2
4	60	80	85	7.55	4.82	57.83	31.55	30.08	2.01
5	120	90	115	10.43	2.59	70.68	30.21	28.18	1.49
6	90	80	120	9.38	2.5	64.62	36.36	37.07	2.02
7	90	80	112	10.77	1.4	70.19	40.56	33.87	2.35
8	90	80	117	10.32	2.03	68.76	39.24	34.83	2.14
9	120	80	140	13.01	5.4	63.43	34.55	33.12	1.82
10	90	70	185	13.43	4.98	54.13	28.55	28.17	1.95
11	60	90	60	5.25	3.79	65.88	28.46	27.7	1.61
12	90	80	113	9.78	2.4	66.13	37.23	36.45	2.09
13	90	90	85	7.18	0.86	75.73	34.02	31.91	1.81

Table 3. Response Surface Methodology (RSM) for drying time, SEC, ΔE, TPC, TFC, AA, and EO of thyme under different drying conditions

EO

For extracting EO, a Clevenger machine and a distillation method were used. The amount of dried thyme used for this research was 30 gr and the amount of water used in each experiment was 500 mL. The duration of essential oil extraction for each treatment was 2 hours after boiling the water. The amount of EO obtained from each treatment was calculated as a percentage[2].

Statistical analysis

The statistical analysis of this research was factorial in the form of a completely random design. A two-factor factorial ANOVA (factors: water temperature and sample weight) including their interaction was conducted in SAS 9.4 at $\alpha = 0.05$. The difference between the mean values was investigated by Duncan's multiple range ($p < 0.05$) comparison method.

Optimization

In this research, in order to design the experiment and evaluate the drying time, SEC, ΔE, AA, TPC, TFC and EO of dried thyme samples, the response surface method (RSM) in the form of central composite design (CCD) was executed using Design Expert 10.0. This design included two independent variables (water temperature and weight of samples) in three levels, in three repetitions and the central point had five repetitions. Table 2 presents the test levels and parameters used in the CCD design. The effects of the WT level (70, 80 and 90 °C) and the SW (60, 90 and 120 g) are presented in Table 3. The multivariate model is in the form of Eq. (24) and according to Rekik et al.,[72] and Meshkat et al.,[74]:

$$y_k = \beta_0 + \sum_{j=1}^{k} \beta_j x_j + \sum_{j=1}^{k} \beta_{jj} x_j^2 + \sum \sum_{i<j}^{k} \beta_{ij} x_i x_j \quad (24)$$

The fitness of the polynomial equation to the responses were estimated using coefficient of determination (R^2). The statistical significance of all polynomial equation terms was determined by calculating the F value at a

significance level of $p < 0.05$[75]. Additionally, 3D response surface plots of the thyme drying parameter analysis were generated using the trial version of Design Expert 10.0 software by Dr. Mohammad Kaveh.

Results and discussion

Kinetics and drying time

Changes in the MR of thyme during the drying process are shown in Figure 2. The MC decreases continuously during the drying process. However, this reduction has been done at higher temperatures and lower weights with a greater slope. This will reduce the drying time and reach the final MC of less than 5% (w.b) sooner. In the early

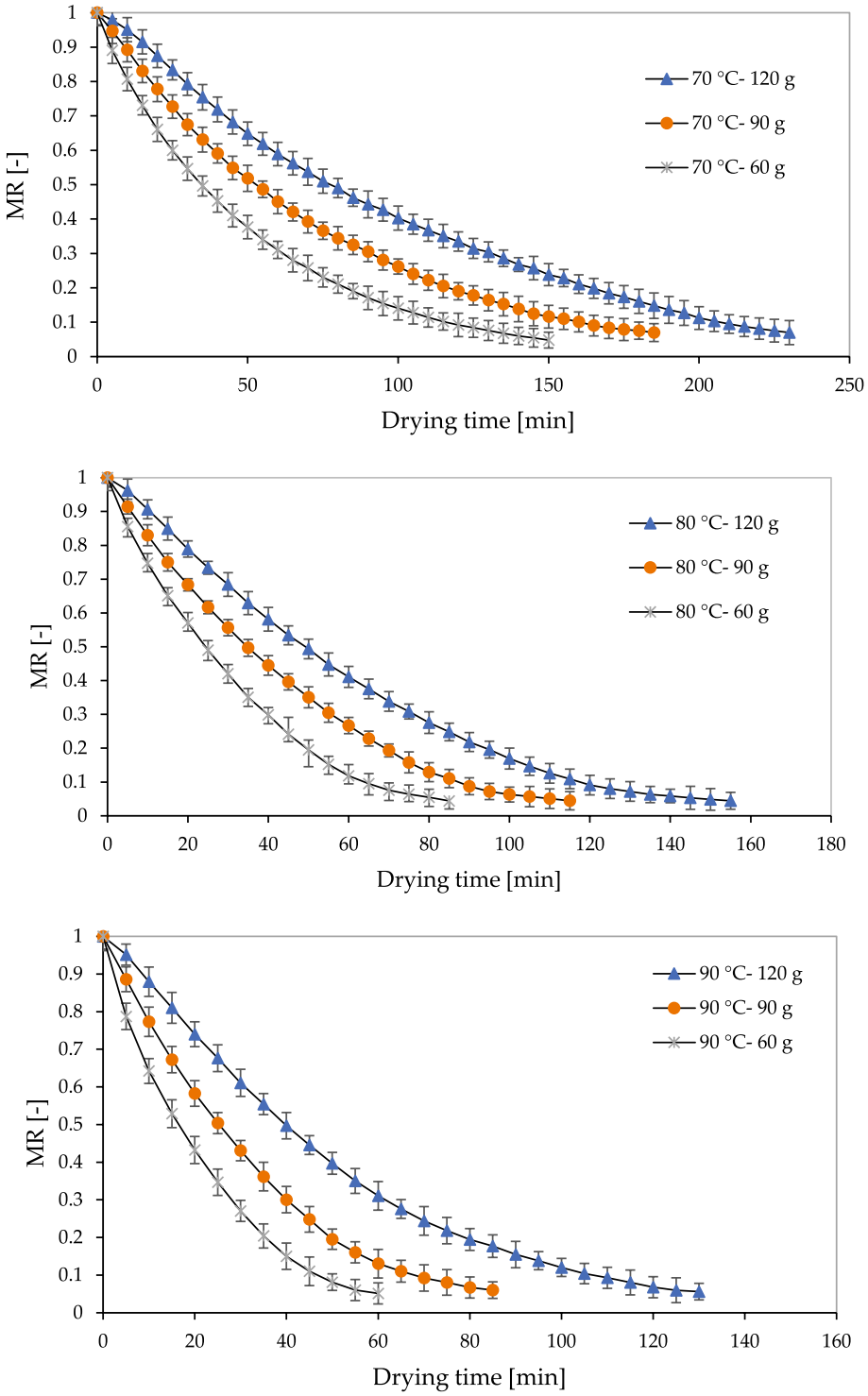

Fig. 2. Moisture ratio variation with drying time during experiments for infrared- refractance window at different air temperature (°C) and weight (g)

Parameters	Time	SEC	ΔE	TPC	TFC	AA	EO
A-Temperature	15504.17**	1.10**	22.12**	3.99×10^{-6**}	30.51**	673.95**	0.05*
B- Weight	6016.47**	1.22**	0.0024^{ns}	1.06×10^{-6**}	8.91*	32.71*	0.020^{ns}
A*B	156.25*	-	0.94^{ns}	8.39×10^{-8ns}	2.74^{ns}	0.12^{ns}	0.001^{ns}
A^2	1437.05**	-	0.42^{ns}	8.77×10^{-6**}	92.66**	19.56*	0.15**
B^2	0.2660^{ns}	-	18.45**	4.24×10^{-6**}	49.47**	133.85**	0.20**
Residual	17.98	0.003	0.22	5.35×10^{-8}	1.06	2.83	0.009
Lack of fit	28.22^{ns}	0.002^{ns}	0.27^{ns}	1.43×10^{-6ns}	0.32^{ns}	0.28^{ns}	0.002^{ns}
Pure error	10.30	0.006	0.18	8.3010^{-8}	1.62	9.46	0.015
C.V	3.39	1.91	3.23	3.92	3.33	2.67	5.14
R^2	0.9946	0.9837	0.9679	0.9857	0.9731	0.9792	0.9041
Adjusted R^2	0.9908	0.9805	0.9450	0.9752	0.9538	0.9643	0.8533
Predicated R^2	0.9651	0.9758	0.8435	0.9695	0.9330	0.9620	0.9188
Model	Quadratic	Linear	Quadratic	Quadratic	Quadratic	Quadratic	Quadratic

Table 4. Means squares and significant level for drying time, SEC, ΔE, TPC, TFC, AA, and EO using the response surface method * Significant at $P< 0.05$, ** significant at $P< 0.01$, ^{ns} not significant at $P< 0.05$

Weight (g)	T (°C)	Drying time (min)	DR (g water/g dry matter)/ min	SEC (kWh/kg)	D_{eff} (m^2/s)
120	70	238.33±3.60 ^{a}	0.005±0.0003 ^{e}	16.61±0.41 ^{a}	1.95×10^{-8}±2.38×10^{-10} ^{g}
	80	146.66±3.60 ^{c}	0.010±0.0004 ^{d}	13.02±0.38 ^{b}	2.73×10^{-8}±5.19×10^{-10} ^{f}
	90	115.00±2.35 ^{d}	0.011±0.0004 ^{cd}	10.43±0.32 ^{c}	3.35×10^{-8}±4.71×10^{-10} ^{e}
90	70	186.66±3.60 ^{b}	0.008±0.0003 ^{d}	13.43±0.39 ^{b}	1.43×10^{-8}±6.61×10^{-10} ^{ef}
	80	116.66±1.36 ^{d}	0.013±0.0004 ^{c}	10.07±0.32 ^{c}	1.69×10^{-8}±3.28×10^{-10} ^{d}
	90	85.00±2.35 ^{e}	0.017±0.0009 ^{b}	7.18±0.31 ^{d}	2.23×10^{-8}±5.66×10^{-10} ^{b}
60	70	155.00±2.35 ^{c}	0.010±0.0004 ^{d}	9.57±0.30 ^{c}	5.06×10^{-9}±4.71×10^{-10} ^{c}
	80	86.66±1.36 ^{e}	0.016±0.0004 ^{b}	7.54±0.27 ^{d}	6.02×10^{-9}±6.13×10^{-10} ^{b}
	90	58.33±1.36 ^{f}	0.021±0.0009 ^{a}	5.25±0.22 ^{e}	7.54×10^{-9}±7.07×10^{-10} ^{a}

Table 5. Effect of different condition on drying time, DR, SEC and D_{eff}, during infrared- refractance window drying

stages of drying, the decrease in moisture occurred more intensively, and with the continuation of the drying process, the slope of the curve decreased. This can be due to the decrease in porosity of the samples, increase in diffusion speed, increase in the surface heat transfer coefficient, and the exit of moisture, especially at higher temperatures during drying, which has been observed by researchers including Kumar et al.,[76] and Pal et al.,[77]. According to ANOVA (Table 4), the effect of water temperature, sample weight, their interaction and square sample weight on drying time was significant (P<0.05). The average drying time obtained from different drying conditions is listed in Table 5 and in that, water temperature of 90 °C and sample weight of 60 g showed the shortest drying time (60 ± 5 minutes) (P<0.01). The drying time was reduced by 60, 54 and 50% by increasing the water temperature from 70 °C to 90 °C for the sample weight of 60, 90 and 120 g, respectively. As the weight of the samples increased, the drying time increased (Figure 3a). Increasing the sample weight slows down the drying process, and the MC decreases with a delay, so water molecules must spend more time to leave the samples. Similar results were reported by Adekanye et al.,[78] and Nurmawati et al.,[79] for Moringa oleifera leaves and mushrooms, respectively.

Drying rate (DR)

According to Figure 4, in the initial stage of the drying process, due to the higher MC on the surface of the bubbles, the DR increased. However in the next stage (decrease speed stage), all the free water on the surface of thyme samples has evaporated as a result of the DR of the product has decreased[48]. The results of the research of Mandale et al.,[49] illustrated that by increasing the drying temperature during beetroot drying, the time required to reach the equilibrium MC decreased. According to Table 6, the WT and SW (P<0.01) and as well as their interaction (P<0.05) had a significant effect on the DR. The average changes in the DR at different water temperature and sample weight are illustrated in Table 5. According to this table, by increasing the WT from 70 to 90 °C, the DR of the thyme raised (P<0.01), that is, DR90°C > DR80°C> DR70°C. Higher temperature leads to a higher rate of heat transfer and moisture diffusion from the inside to the surface to evaporate the samples[49]. Whereas, increasing the sample weight from 60 to 120 g caused a reduce in the DR of the product (P<0.05). At smaller weight, moisture transfer occurs more quickly, thus improving DR. Therefore, a higher DR was observed in lower weights while a lower drying rate was observed for higher weights, i.e. DR60g> DR90g> DR120g

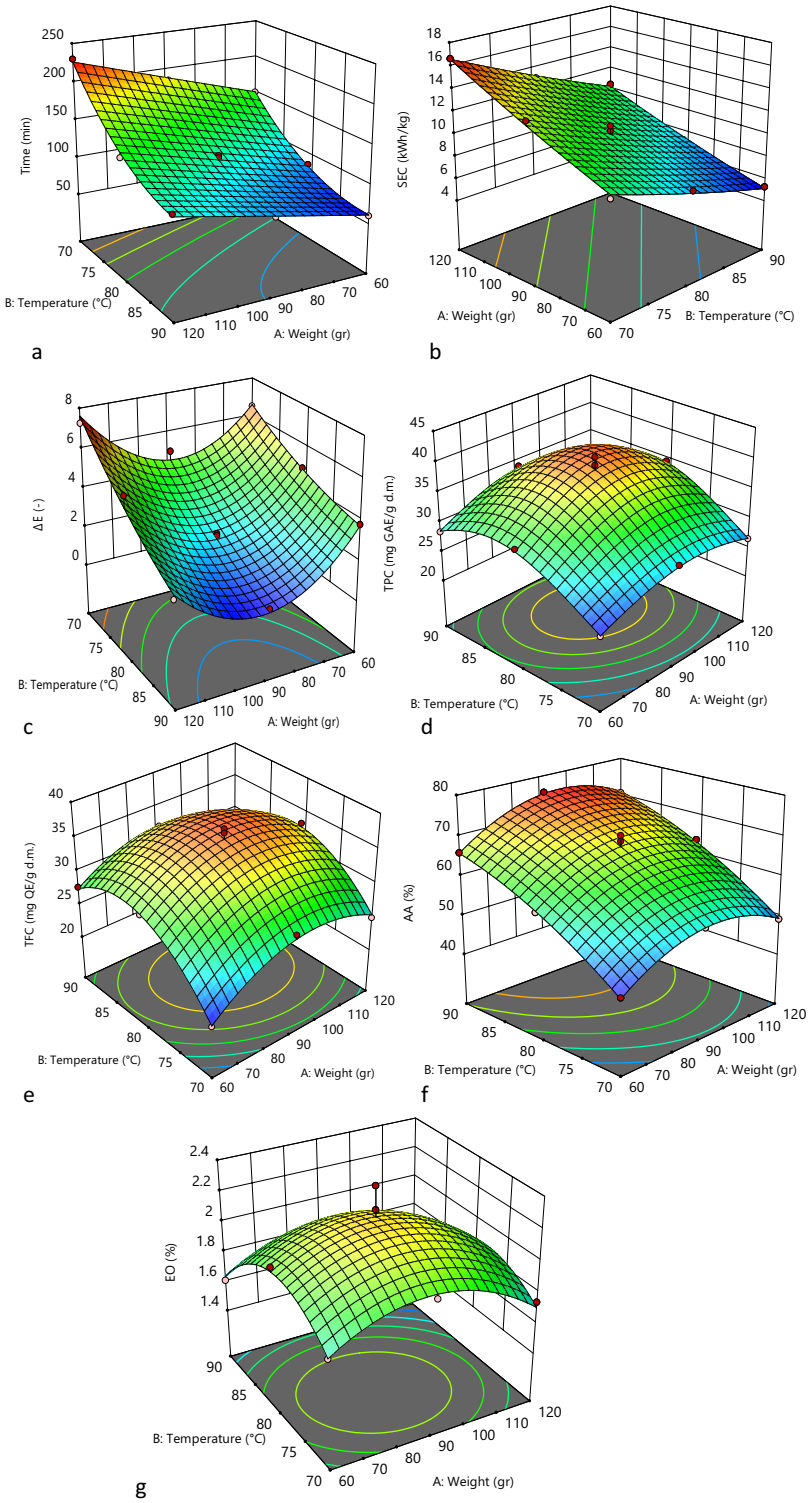

Fig. 3. Response surface for different properties (drying time (**a**), SEC (b), ΔE (**c**), TPC (**d**), TFC (**e**), AA (**f**) and EO (**g**) of dried thyme at different temperatures and weight. Figure 3 is extracted from Design Expert software' this clarification in the main manuscript.

Modeling

Drying data was utilized to describe the IR-RW drying kinetics of thyme. The experimental data were fitted using nonlinear regression analysis with eight frequently used model equations. By calculating the amount of MR during the drying process of thyme, by means of kinetic models, the results for each model were examined and compared (Table 7). The modeling results showed that the best model for thyme drying process with the highest fit, the highest value of the R^2 and the least RMSE and χ^2 is the model of Midilli et al. In (Table 7 and 8), sum of

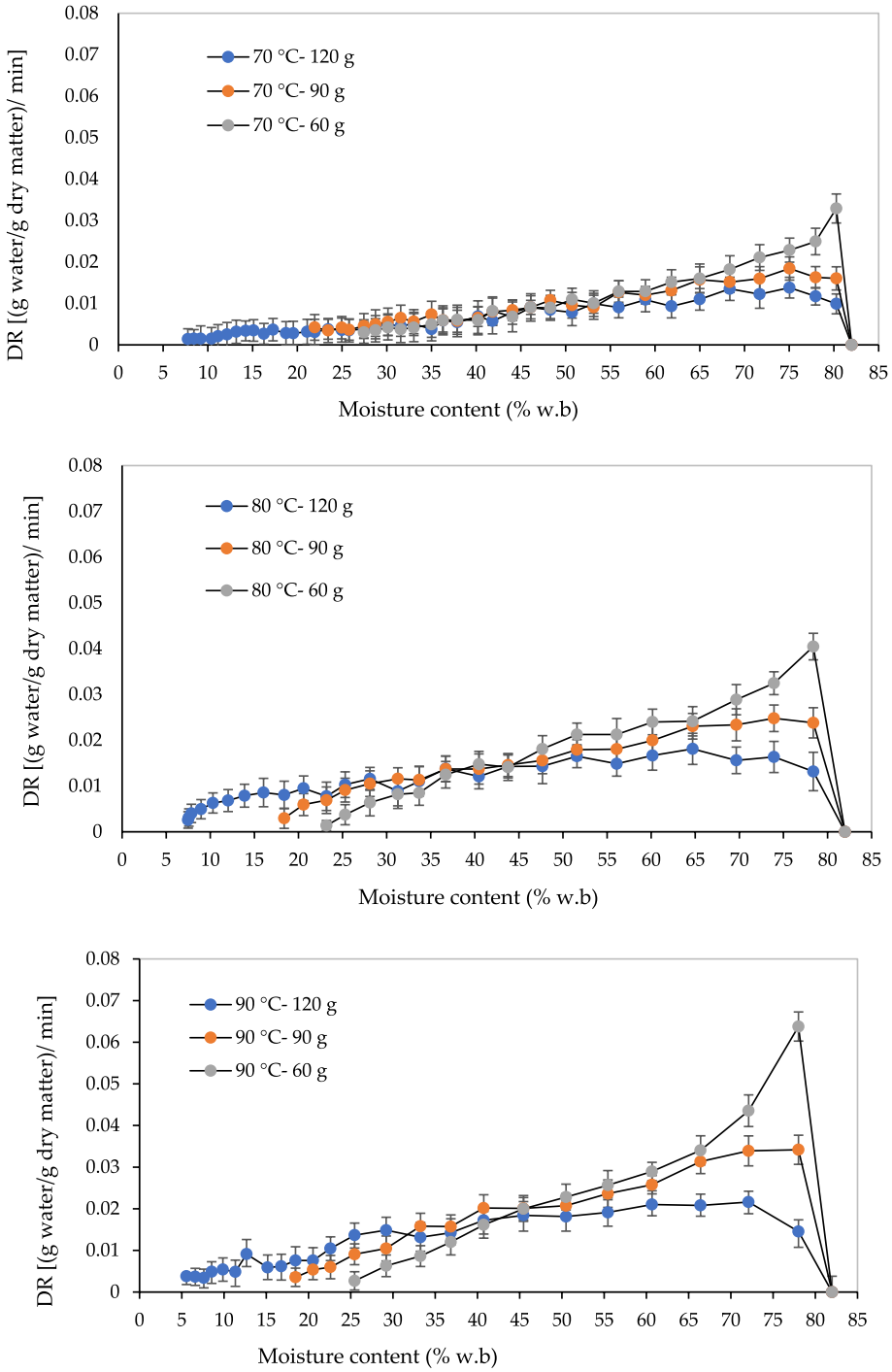

Fig. 4:. Drying rates of the thyme samples for infrared- refractance window at different air temperature (°C) and weight (g)

squares of error (RMSE), coefficient of determination (R^2) and chi-square (χ^2) as well as constant coefficients of Midilli et al.'s model (n and k) for different drying conditions of thyme samples are reported. In this research, the values of RMSE, R2 and χ^2 were obtained in the range of 0.00124 to 0.00689, 0.9992 to 0.9999, and 0.00008 to 0.00093, respectively. The model parameter k varied from 0.0033 to 0.0112 for a variation in temperature from 70 to 90 °C for 60 to 120 g sample weight case. Further, n varied to a lesser extend (0.9998 to 1.325) with sample weight (60 to 120 g). In addition, the changes in parameters b and a under different conditions were determined to be in the range of -0.00067 to 0.000072 and 0.9961 to 1.0005, respectively. According to Table 8, as the drying air temperature increases, the k value of the model of Midilli et al. also increases. Kalsi et al.[71] stated that the drying curve becomes steeper with increasing k value, which means faster drying. Uribe et al.[47] studied the drying kinetics of physalis by the RW method under temperatures ranging from 50 to 90°C. Based on their

Parameters	df	DR	D_{eff}	L*	a*	b*	Chroma	BI
A-Temperature	2	0.0001^{**}	$1.56\times10^{-16**}$	14.31^{**}	1.68^{**}	30.7^{**}	32.15^{**}	2276.0^{**}
B- Weight	2	0.0001^{**}	$3.78\times10^{-16**}$	14.26^{**}	3.88^{**}	16.61^{**}	18.61^{**}	1198.0^{**}
A*B	4	0.000006^{*}	3.32×10^{-18ns}	0.77^{**}	0.25^{*}	1.43^{**}	1.47^{**}	101.80^{ns}
Error	16	1.97×10^{-6}	1.97×10^{-18}	0.088	0.072	0.2309	0.2241	37.1
C.V		10.9	6.5	0.9	11	2.8	2.73	7.88

Table 6. Means squares and significant level for DR, D_{eff}, L*. a*, b*, and Chroma * Significant at $P< 0.05$, ** significant at $P< 0.01$, ns not significant at $P< 0.05$

Model name	Tempera-ture (°C)	R2			χ^2			RMSE		
		60 g	90 g	120 g	60 g	90 g	120 g	60 g	90 g	120 g
Page	70	0.9991	0.9984	0.9993	0.00110	0.00249	0.00098	0.00761	0.00926	0.00714
	80	0.9989	0.9979	0.9961	0.00142	0.00309	0.00450	0.00870	0.00969	0.02350
	90	0.9969	0.9991	0.9986	0.00391	0.00119	0.00229	0.01251	0.00777	0.00912
Wang and Singh	70	0.9891	0.9865	0.9777	0.01029	0.01325	0.02398	0.05135	0.05502	0.09654
	80	0.9799	0.9699	0.9785	0.01999	0.03898	0.02245	0.08692	0.17694	0.09358
	90	0.9826	0.9901	0.9873	0.01739	0.00942	0.01239	0.06728	0.04321	0.05465
Newton	70	0.9698	0.9679	0.9825	0.03905	0.04025	0.01742	0.17951	0.1812	0.06861
	80	0.9711	0.9864	0.9844	0.03666	0.01342	0.01411	0.16987	0.05534	0.05812
	90	0.9802	0.9799	0.9768	0.01967	0.02002	0.02451	0.08342	0.08725	0.09754
Verma et al	70	0.9869	0.9962	0.9929	0.01293	0.00431	0.00775	0.05467	0.02228	0.03725
	80	0.9899	0.9819	0.9944	0.00956	0.01782	0.00613	0.04368	0.07293	0.03388
	90	0.9926	0.9899	0.9893	0.00805	0.00959	0.01002	0.03912	0.04390	0.05124
Logarithmic	70	0.9961	0.9979	0.9953	0.00439	0.00305	0.00531	0.02292	0.00659	0.03233
	80	0.9978	0.9938	0.9949	0.00314	0.00711	0.00583	0.00972	0.03458	0.03309
	90	0.9959	0.9899	0.9929	0.00469	0.00961	0.0772	0.02999	0.04379	0.03687
Henderson and Pabis	70	0.9712	0.9821	0.9788	0.03654	0.01768	0.02281	0.16584	0.07215	0.09211
	80	0.9760	0.9789	0.9723	0.02578	0.02221	0.03215	0.12451	0.09021	0.15480
	90	0.9800	0.9842	0.9833	0.01992	0.01432	0.01698	0.08524	0.05839	0.06542
Midilli et al.,	70	0.9994	0.9998	0.9999	0.00086	0.00014	0.00008	0.00495	0.00245	0.00124
	80	0.9995	0.9998	0.9996	0.00077	0.00037	0.00069	0.00449	0.00280	0.00412
	90	0.9992	0.9997	0.9997	0.00093	0.00061	0.00052	0.00689	0.00355	0.00329
Two-term	70	0.9969	0.9978	0.9991	0.00388	0.00311	0.00112	0.01241	0.00967	0.00769
	80	0.9954	0.9989	0.9990	0.00521	0.00142	0.00129	0.03215	0.00869	0.00842
	90	0.9982	0.9994	0.9986	0.00279	0.00093	0.00129	0.00929	0.00569	0.00919

Table 7. Compared values of statistical parameters of empirical models of drying of thyme in infrared-refractance window

Weight sample (g)	Drying temperature (◦C)	a	k	n	B
60	70 °C	0.9965	0.0093	1.0158	-0.00067
60	80 °C	0.9971	0.0095	1.0587	0.000029
60	90 °C	0.9961	0.0112	0.9998	-0.00018
90	70 °C	0.9997	0.0051	1.3251	0.000059
90	80 °C	1.0001	0.0065	1.0723	0.000034
90	90 °C	0.9978	0.0066	1.1253	0.000062
120	70 °C	1.0005	0.0043	1.1954	0.000072
120	80 °C	0.9974	0.0048	1.2452	0.000045
120	90 °C	0.9983	0.0053	1.0985	0.000038

Table 8. The coefficients and statistics of the Midilli et al., models for different drying air temperatures and thyme weight sample

results, the Midilli & Kucuk model described the drying behavior of physalis well. Ayala-Aponte et al.[80] modeled the drying of Aloe vera gel slabs in a window dryer in a study. Experiments were conducted in the temperature range of 60-90 °C and slab thicknesses of 5 and 10 mm. The Midilli & Kucuk model described the behavior of the drying process of Aloe vera gel slabs better than other models.

D_{eff}

According to ANOVA (Table 6), water temperature and sample weight have a significant effect on thyme D_{eff} ($P<0.01$). According to the results (Table 5), the highest and lowest values of D_{eff} were 3.01×10^{-8} and 8.67×10^{-9} m^2/s, respectively, and the highest value was recorded at a WT of 90 °C and a SW of 60 g, while its minimum value was recorded at 70 °C and 120 g. According to Table 5, by increasing WT and reducing the SW, the D_{eff} has increased, which has led to the acceleration of the exit of moisture to the surface of the thyme samples, and as a result, the drying speed has raised[81]. The amount of D_{eff} for drying food has been reported in the range of 10^{-12} to 10^{-7}[61] and the results of this study are also in the same range. Karami et al[2] obtained D_{eff} values for dried thyme in the solar-electric dryer method in the range of 1.23×10^{-10} to 2.17×10^{-10} m^2/s. Also, the D_{eff} in the study of Turan and Firatligil,[82] for dried thyme in the hot air technique was reported from 2.59×10^{-9} to 1.28×10^{-8} m^2/s.

SEC

The results of analyzing the effect of WT and SW on SEC and comparing its averages are shown in Tables 4 and 5, respectively. As can be seen in Table 4, the change of WT and SW had a significant effect on SEC ($P<0.01$), and with rising WT and reducing SW, SEC decreased. However, the interaction and quadratic effect of WT and SW on energy was not significant. For example, for the SW of 60 g, the average SEC of the drying process of thyme samples in the IR-RW dryer at WT of 70, 80 and 90 °C was determined using experimental data and Eq. (16) and 9.57, 7.54 and 5.25 kWh/kg were obtained, respectively. Similar results were announced by researchers in RW such as Zalpouri et al.,[50] for coriander (7.88 to 9.10 kWh/kg), Rajoriya et al.,[15] for drying banana (2.48 to 2.80 kWh/kg), and Seyfi et al.,[12] for drying Aloe vera gel (4.31 to 7.31 kWh/kg). Significantly, SEC was the lowest in higher water temperature for all different weights of thyme ($P<0.01$) (Figure 3b). When the temperature raised from 70 to 90 °C and from 80 to 90 °C, SEC was decreased 45.10 and 30.30% for 60 g, 46.50 and 28.6% for 90 g, 37.34 and 19.00% for 120 g, respectively. Reducing the process time at higher WT is the most important reason for decreasing the SEC of the process. According to the average comparison Table 5 and (Figure 3b), the SW of 60 g dried at 90 °C has the minimum SEC value of 5.25 kWh/kg, while the SW of g 120 dried at 70 °C has the maximum SEC value of 16.61 kWh/kg. The SEC values reported in this study for the IR-RW method were obtained at a laboratory scale. On the one hand, heat recovery management, insulation quality, control strategy (e.g., variable speed pumps/fans), and laboratory environment can reduce SEC compared to laboratory units. On the other hand, start/stop cycles, partial loads, and maintenance modes may increase SEC. Therefore, our SEC values should be considered as a laboratory benchmark rather than direct industrial surrogates.

CO_2

In Figure 5, the effect of water temperature and sample weight on CO_2 from different power plants using different fuels is shown. According to Figure 5, the amount of CO_2 varied from 0.426 to 21.25 kg/kg water. As it is clear from the figure, the amount of CO_2 reduced with the increase in the inlet WT, while this amount raised with the increase in the weight of the samples. The highest amount of CO_2 was obtained in G-T power plant with G-O fuel and the lowest amount of CO_2 was obtained in S-P power plant with N-G fuel. The reason for the reduction of GHG emissions can be seen in the reduction of SEC and drying time during the drying process, due to the increase in moisture evaporation at high temperatures and low weights[67]. In addition, at low temperatures, the dissolved solids along with water are placed on the surface layer of the samples and the phenomenon of surface hardening occurs. As a result, the tissue has become stiffer and more energy is needed for drying. As

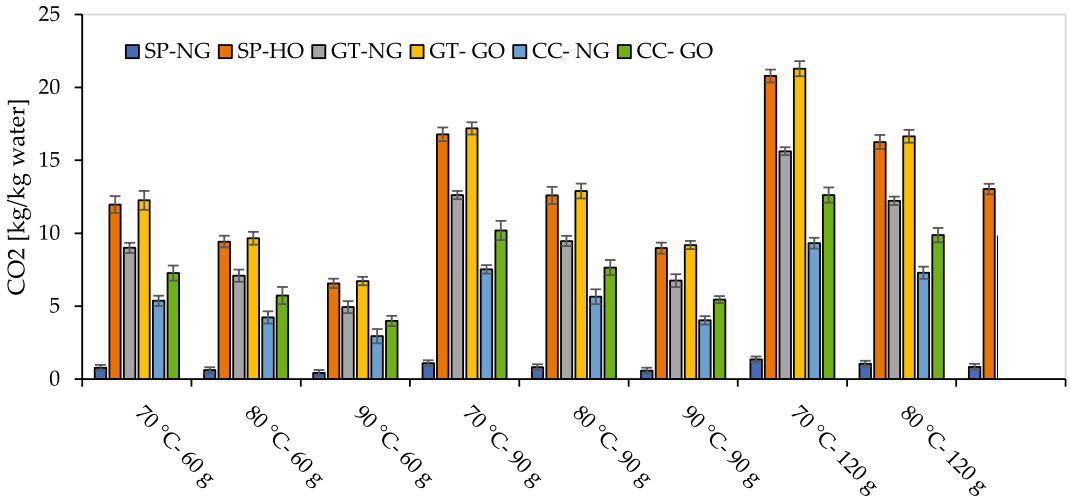

Fig. 5. CO2 emissions from different power plants and fuel under various drying condition.

a result, more CO_2 emissions is produced. Seyfi et al.,[12] dried Aloe vera gel using solar- RW and observed that increasing WT decreased CO_2 emission. Baeghbali et al.,[42] reported that the release of CO_2 during the drying of pomegranate juice by the RW method was 3.45 kg.

Activation energy

To determine the Ea, different values of Ln (D_{eff}) were drawn apposed to the inverse of the absolute temperature within the product in the process of drying (1/T). The Ea values varied from 20.71 to 31.17 kJ/mol (Table 9). The Ea gained in the present study is within an acceptable area, because according to Cunha et al.,[61] the Ea values for all food, fruit, vegetables and medical plant are between 12.7 and 110 kJ/mol. Ea for physalis (29.49 kJ/mol), avocado (32.06 kJ/mol) and *Curcuma longa* L. (47.05 kJ/mol) in the RW method, have been reported in the study of Uribe et al.,[47], Nguyen et al.,[48] and Cunha et al.,[61], respectively.

Thermodynamic

According to Table 9. The effect of temperature on ΔH was not significant ($p<0.01$), but it was significant on ΔS. In addition, the effect of weight on both parameters (ΔH and ΔS) was significant ($p<0.05$). On the other hand, the effect of temperature and weight on ΔG was significant ($p<0.05$). Table 9 shows the ΔH, ΔS and ΔG obtained from the drying of thyme. ΔH values ranged from 17.69 to 28.15 kJ/mol. similar results were found by Cunha et al.,[61] in drying Curcuma longa L. and at water temperature between 70 and 90 °C, with ΔH in the range of 44.026 to 44.193 kJ/mol. According to Table (9), ΔH values are inversely proportional to temperature and decreases with increasing temperature, while it also decreases with decreasing weight of samples. Decreasing enthalpy shows that less energy is required for drying at higher WT and lower SW. The enthalpy values (ΔH) in this study were obtained as positive, which according to de Vilela Silva et al.,[83] indicates an endothermic process with heat absorption (endergonic reactions) which is related to the increase in the partial pressure of water vapor in thyme and it is caused by increasing the drying air temperature[84]. Other studies on drying black rice[85], Uzun pistachios[60] and peppers[84] confirm these results.

According to Table 9, it can be seen that ΔS, which is related to the degree of disorder of the system, behaved similarly to enthalpy (ΔH), which slightly reduces with the increase in the WT. This behavior indicates less mixing of water molecules and more order between these molecules in the system[84]. The highest and lowest entropy values were -0.1181 and -0.1490 kJ/mol K, respectively. Santos et al.,[86] also identified negative entropy values in the process of drying mango peels with values of -0.3098 to -0.2468 kJ/mol K. Similar behavior is also observed in the drying of peppers[84], wheat[87] and pineapple[88].

According to Table 9, the highest amount of Gibbs free energy (73.04 kJ/mol) was acquired at 90 °C of water temperature and the weight was 120 g, and the lowest value (67.69 kJ/mol) was gained at 70 °C of WT and SW 60 g. As the WT increased and the sample weight decreased, the amount of ΔG increased. ΔG is the total amount of energy involved in the system and can characterize the drying process as spontaneous or non-spontaneous and shows the amount of water attached to the product. Values greater than zero ($\Delta G>0$) mean that the drying process was not spontaneous. Several studies were conducted on the thermodynamic properties of agricultural products, which showed that an increase in WT causes an increase in ΔG and the non-spontaneity of the process. The results related to the drying of *Curcuma longa* L. by Cunha et al.,[61], who showed that the ΔG value increased from 122.75 to 127.33 kJ/mol by raising the WT from 70 to 90 °C. Also, Santos et al.,[89] detected an increase in ΔG in the drying of guava slices with raising temperature from 50 to 90 °C, with values from 75.13 to 80.95 kJ/mol.

Color

The color of the surface of the dried samples is one of the main quality parameters that determines the acceptance of the product. Process variables, including water temperature and sample weight, affect the color of the dried product. The average index of brightness, redness and yellowness of fresh thyme samples was 35.9, 1.28 and 15.2, respectively. Table 6 illustrates the effect of WT and SW on the color indices of dried thyme samples. Based on the results reported in this table, WT and SW have a significant effect on the change of color indices (a*, b*, L*, Chroma) of dried thyme samples ($P< 0.05$). The average index of brightness, redness, and yellowness of dried thyme samples was in the range of 30.6- 36.01, 1.47- 3.33, and 13.37- 20.14, respectively.

Wight (g)	Temperature (°C)	Ea (kJ/mol)	R^2	ΔH (kJ/mol)	ΔS (kJ/mol K)	ΔG (kJ/mol)
60	70	31.17	0.9701	17.86 ^{c}	-0.1452 ^{c}	67.69 ^{i}
	80			17.77 ^{c}	-0.1471 ^{c}	69.75 ^{f}
	90			17.69 ^{c}	-0.1490 ^{c}	71.81 ^{c}
90	70	25.79	0.9945	22.94 ^{b}	-0.1320 ^{b}	68.23 ^{h}
	80			22.85 ^{b}	-0.1343 ^{b}	70.30 ^{e}
	90			22.77 ^{b}	-0.1366 ^{b}	72.38 ^{b}
120	70	20.71	0.9997	28.32 ^{a}	-0.1181 ^{a}	68.86 ^{g}
	80			28.23 ^{a}	-0.1209 ^{a}	70.95 ^{d}
	90			28.15 ^{a}	-0.1236 ^{a}	73.04 ^{a}

Table 9. Activation energy and thermodynamic properties of the thyme drying process with infrared-refractance window. Values are mean ± SD (n = 3). Within each column, different superscript letters indicate statistically significant differences according to Duncan's multiple range test ($p < 0.05$)

The results of the color analysis of dried thyme samples show that L* value is lower than fresh samples in all different weights ($p<0.05$). According to Table 10, the closest L* to fresh thyme leaves was recorded at water temperature of 90 °C and sample weight of 90 g. According to Table 10, the increase in temperature increases the value of L*. Therefore, the high water temperature in the refractance window method preserved the color of the dried samples better. Similar results were reported in the study of Selvakumarasamy et al.,[90] for drying *Costus pictus* rhizomes. On the other hand, medium weights (90 g) had higher L value changes than 60 and 120 g weights. Since the color of the thyme samples became dark green during drying, the index a* (expressing the amount of redness/greenness of the product) improved compared to the fresh samples. Also, the values of a* reduce with raising temperature. In addition, this value showed a higher value in higher weights (120 g). The b* value (expressing the yellow/blue value of the product) of thyme samples improved after drying because the yellowness of thyme samples decreased drastically during drying. Also, the value of b* in all treatments reduced with raising temperature. The reason can be attributed to the Maillard browning reactions and browning index[91].

Color difference (ΔE) measured the overall color change of thyme samples and is an important parameter to evaluate the color of the sample during the drying process. The lowest value of ΔE indicated the better quality of the dried sample. As shown in Table 10, with the increase of WT, the total color change has decreased significantly ($P<0.05$). The thyme dried at 70 °C showed the maximum amount due to prolonged drying time (Figure 3c). Similar results have been reported for drying Salicornia fruticose[92].

The Chroma parameter shows the level of color stability and the smaller the difference with the new sample, the more suitable the product is. According to the calculated value of this parameter in Table 10, it is clear that the sample dried in WT of 90 °C and SW of 90 g shows the least difference with the fresh sample. The Chroma value for dried thyme was in the range of 14.44 to 20.40.

According to Table 10, it is clear that the color index (BI) decreased with increasing water temperature and decreasing sample weight, indicating less browning under faster drying conditions. According to these results, the lowest BI value was obtained at 90 °C and SW of 90 g.

Rehydration ratio

Drying causes changes in the structure and texture of plant material, and hence causes the irreversibility to its original properties; Therefore, RR is known as an indicator of the severity of the drying process and damage to food texture[73,93]. Figure 6 shows the process of increasing RR in dried samples of thyme leaves at WT of 70, 80 and 90 °C and SW of 60, 90 and 120 g as a function of time; as shown in Figure 6, with the increase of rehydration time, RR increased, but after a certain time, this value remained constant. Similar results have been reported in the literature for different crops, for example, wormwood[73] and red Cabbage[94]. The high rate of RR at the beginning of the process may be related to the rapid absorption of water in the capillaries and cavities near the surface[95]. Subsequently, the water absorption rate decreased due to the filling of free capillaries and intercellular spaces. Also, with the increase in WT, due to less damage to the cell structure, it showed faster absorption, so the amount of RR increased. Doymaz,[96] obtained similar results when drying thyme and stated that RR improves at higher temperatures due to the effect of temperature on the cell wall and tissue. Based on the observations in Figure 6, the results show that the highest RR was related to the samples dried at 90°C and weighing 60 g (RR=3.88). Based on the results reported in Figure 6, increasing the weight of the samples has a significant effect on the RR of the dried thyme. The RR decreased with the increase in the SW. When the SW was 120 g, the RR decreased significantly

TPC

Phenolic compounds are an important part of the effective substances of medicinal plants, which are influenced by environmental factors, growth conditions and post-harvest operations[97]. In the current research, the trend of changes in TPC of thyme under the influence of sample weight and water temperature is shown in Table 4. As can be seen, the WT, SW and square the WT and SW showed a significant effect on the TPC (Table 3- $P<0.01$), While the interaction effect of the WT and SW was not significant on the TPC (Table 3- $P<0.05$). The TPC of dried thyme varied from 24.15 to 38.45 mg GAE/100 g d.m. As the SW increases up to 80 g, TPC has an upward trend, while at higher weights (above 90 g), the TPC of the samples has a downward trend ($P<0.01$) (Table 11-

Weight (g)	Temperature (°C)	L*	a*	b*	ΔE	Chroma	BI
120	70	31.27±0.21 ^{ef}	3.52±0.08 ^{ef}	21.21±0.45 ^{a}	7.93±0.33^{a}	21.50±0.46^{a}	111.29 ^{a}
	80	32.65±0.19 ^{d}	3.44±0.27 ^{d}	18.71±0.06 ^{b}	5.27±0.14^{c}	19.03±0.06^{b}	87.70 ^{b}
	90	33.70±0.11 ^{c}	2.40±0.07 ^{c}	16.08±0.08 ^{d}	2.62±0.09^{e}	16.26±0.06^{d}	67.22 ^{d}
90	70	32.22±0.24 ^{d}	2.23±0.11 ^{d}	17.63±0.10 ^{c}	4.52±0.18^{c}	17.77±0.09^{c}	79.89 ^{bc}
	80	34.25±0.20 ^{b}	1.58±0.08 ^{b}	16.24±0.26 ^{d}	2.00±0.26^{e}	16.32±0.26^{d}	64.91 ^{d}
	90	35.77±0.09 ^{a}	1.65±0.12 ^{a}	14.27±0.19 ^{e}	1.03±0.21^{f}	14.37±0.17^{e}	52.34 ^{e}
60	70	30.82±0.09 ^{f}	2.84±0.07 ^{f}	18.21±0.32 ^{bc}	6.12±0.21^{b}	18.43±0.32^{bc}	90.40 ^{b}
	80	31.54±0.07 ^{e}	2.20±0.07 ^{e}	16.39±0.03 ^{d}	4.61±0.08^{c}	16.53±0.03^{d}	74.73 ^{cd}
	90	32.39±0.09 ^{d}	1.94±0.04 ^{d}	15.61±0.14 ^{d}	3.59±0.08^{d}	15.73±0.13^{d}	67.03 ^{d}

Table 10. Impact of air temperature and weight of sample on L*,a*,b*, ΔE and Chroma of thyme during infrared- refractance window drying Values are mean ± SD (n = 3). Within each column, different superscript letters indicate statistically significant differences according to Duncan's multiple range test ($p < 0.05$).

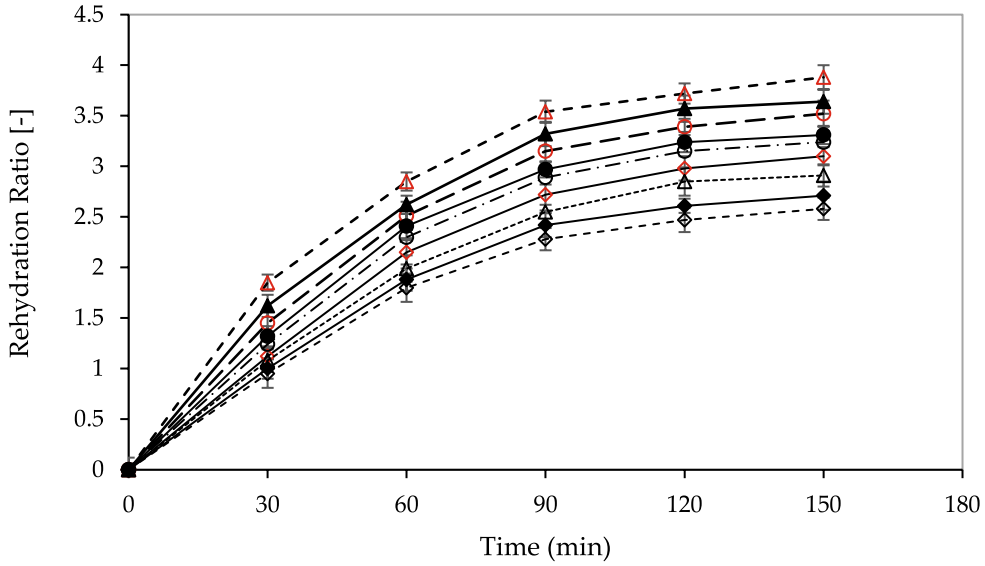

Fig. 6.. Plots of the rehydration rates of thyme at different water temperatures and weight sample. ◊ (70 °C- 120 g), Δ (70 °C- 90 g), ○ (70 °C- 60 g), ◆ (80 °C- 120 g), ● (80 °C- 90 g), ▲ (80 °C- 60 g), ◊ (90 °C- 120 g), ○ (90 °C- 90 g), Δ (90 °C- 60 g).

Weight (g)	Temperature (°C)	TPC (mg GAE/100 g d.m)	TFC (mg QE/100 g d.m)	AA (%)	EO (%)
120	70	26.55±0.78 ^{ef}	24.94±0.65 ^{e}	49.11±1.18 ^{ef}	1.67±0.04^{ed}
	80	34.58±0.66 ^{b}	33.12±0.65 ^{ab}	63.41±1.15 ^{c}	1.81±0.05^{bcd}
	90	30.18±0.75 ^{d}	28.18±0.61 ^{d}	70.67±1.57 ^{ab}	1.50±0.03^{e}
90	70	28.57±0.73 ^{de}	28.15±0.0.70 ^{d}	54.11±1.78 ^{ed}	1.95±0.05^{bc}
	80	38.45±0.98 ^{a}	35.47±0.75 ^{a}	67.40±1.31 ^{bc}	2.19±0.07^{a}
	90	34.02±0.65 ^{bc}	31.91±0.65 ^{bc}	75.71±1.35 ^{a}	1.81±0.05^{bcd}
60	70	24.12±0.54 ^{f}	21.14±0.56 ^{f}	45.49±1.65 ^{f}	1.77±0.04^{cd}
	80	31.54±0.70 ^{cd}	30.08±0.80 ^{cb}	57.81±0.98 ^{d}	2.02±0.05^{ab}
	90	28.45±0.75 ^{ed}	27.70±0.65 ^{d}	65.87±1.22 ^{bc}	1.60±0.04^{ed}

Table 11. Impact of air temperature and weight of sample on TPC, TFC, AA and EO of thyme during infrared- refractance window drying

Figure 3d). The reduction of TPC in higher weights may be due to the enzymatic processes that occur during the drying process. Higher weights cannot deactivate decomposing enzymes such as polyphenol oxidase due to the longer drying process. As can be seen, lower sample weight (60 g) have a more severe destructive effect than other weights on the amount of total TPC. Also, with the increase in WT, the TPC of thyme first goes up and then goes down. As the WT increases from 70 to 80 °C, the share of TPC increases due to moisture evaporation, but at WT higher than 80 °C, due to the destructive effect of heat, the amount of TPC decreases with increasing temperature. TPC is one of the heat-sensitive compounds that oxidizes quickly so that it begins to decompose and decrease rapidly with the increase in WT. Pal et al.,[77] reported that the decrease in TPC in aonla samples under high and low heat treatments was due to less inactivation of oxidative enzymes and this condition causes the Maillard reaction and thus releases phenolic compounds.

TFC

The results of this realization showed that the effect of WT, SW and square the WT and SW on TFC was significant (P≤0.05- Table 4). The highest TFC for thyme was observed at a SW of 90 g and a WT of 80 °C, while the lowest was obtained at a SW of 60 g and a WT of 70 °C (Table 11- Figure 3e). The amount of TFC in the range of 14.21 to 35.47 mg QE/100 g d.m. was calculated (P≤0.01). This is explained by the possibility that the long heating time decomposes the flavonoids. In addition, flavonoid molecules are heat-sensitive bioactive chemicals with unstable chemical properties, so high temperatures may accelerate flavonoid degradation[98]. Hassan and Koca[99], found that the amount of TFC for dried autumn olive berries increases first and then decreases with increasing temperature.

AA

The change process of thyme AA during IR-RW drying is shown in Table 11 and Figure 3-f. Also, the results of statistical analysis on antioxidant activity showed that the main parameters have a significant effect on it (Table 3- $P<0.05$). According to Table 11 and Figure 3-f, the amount of AA increased with the rise in the weight of the samples up to 90 g, and then with the increase in the SW, there is a downward trend, but with the increase in the WT, it shows an increasing trend. Applying a higher WT leads to an increase in the AA of the samples. The amount of AA of the samples is in the range of 45.48-75.73%. Similar results were reported for drying papaya[100] and beetroot[49] in RW dryer. The results of this study proved that increasing the WT had a positive correlation with antioxidant properties. Increasing the WT led to a decrease in drying time, thereby ensuring the preservation of AA. As stated by Padhi et al.,[101] in drying banana in RW dryer. As can be seen in Table 11 and Figure 3-f, with the increase in the SW, the AA of the dried samples first has an upward trend and then a slight decrease in the weight range above 90 g. In higher SW, it needs more time to reach the required moisture, for this reason, it is subjected to heat treatment for a longer period of time

EO extraction

The average values of essential oil extracted from fresh and dried thyme leaves are shown in Table 11. As can be seen, the effect of WT had a significant effect on the EO percentage of thymes, but the interaction effects and weight sample were not significant ($P<0.05$) (Table 4). The maximum amount of EO (2.20 %) was obtained from dried leaves with WT of 80 °C and SW of 80 g and the lowest amount (1.49 %) was obtained from dried samples with WT of 90 °C and SW of 120 g. As it is clear from the Table 11 and the figure of the RSM (Figure 3-g), at all levels of SW (from 60 to 120 g), the maximum amount of EO was obtained from the dried leaves at 80 °C. As the WT increased from 80 to 90 °C, the EO value of the leaves decreased continuously, which was probably due to the increase in the temperature of the samples and the acceleration of the evaporation of EO from thyme. Similar results were reported by Setareh et al.,[102] regarding the negative effect of high temperatures on the amount of lemongrass EO. They also concluded that medium water temperatures can produce the highest amount of EO. According to Figure 3g, it can be found that 90 g sample weight is more effective in maintaining the EO of the samples compared to 120 g and 60 g sample weight. The lowest amount of EO was obtained in the weight of 120 g, which is due to the longer exposure of the samples to heat, which leads to the destruction of thyme compounds.

Optimization

The drying process should be done in such a way that, in addition to preserving the food from spoilage, the quality indicators of the product, such as color, taste, aroma and texture, are harmed as little as possible. The apply of RW technique can be effective in the drying process of medicinal plants due to small changes in the aroma, taste and quality of the final product. The goal of this optimization was to produce a sample with higher AA, TPC, TFC and EO activity, as well as lower drying time, SEC and ΔE. Figure 7 presents the obtained values for the desirability of each control factor, response variables and combined optimization. As shown, the combined utility is about 0.807. The utility function for the control factors including weight of samples (A) and water temperature (B) is equal to 1 because the values are in the optimization range. Table 12 summarizes different optimal values for dried thyme in IR-RW. Among the optimal values, the obtained predicted optimal variables are: drying time 91.003 min, SEC (8.37 kWh/kg), color changes (1.42), AA (71.68%), TPC (37.93 mg GAE/100 g d.m), TFC (35.11 mg QE/100 g d.m) and EO (2.04%). Finally, the highest level of favorability (0.807) was selected for water temperature (85.02 °C) and sample weight (86.10 g).

Conclusions

Infrared-assisted refractance window drying of thyme across 70–90 °C and 60–120 g achieved fast moisture removal with favorable energy and quality outcomes. The Midilli model best represented thin-layer kinetics (R^2: 0.9992–0.9999; RMSE: 0.00124–0.00689; χ^2: 0.00008-0.00093). Increasing water temperature increased DR, Deff and RR, and reduced time, SEC, CO_2, ΔE, and BI. Regardless of the weight of the samples, the qualitative parameters showed that the samples dried at 80 °C had the highest TPC (38.45 mg GAE/100 g d.m.), TFC (35.47 mg QE/100 g d.m.) and EO (2.19%). Finally, the optimal point for the independent parameters for the process of drying thyme was calculated at the bath water temperature of 85.02 °C, and the sample weight of 86.10 g with a desirability rate of 0.807. These findings are useful for the development of new products from dried thyme using the IR-RW method. This study also showed that IR-RW drying technology as an economically profitable technology through reducing drying time, less energy consumption, reducing long-term heat treatment, improving quality properties, better maintaining bioactive properties and essential oil efficiency, and also it is affordable for consumers. On other hand, the results of this study were obtained from an IR-RW laboratory unit; Heat/mass transfer strategies and scale -dependent control may change SEC and quality results. Methodological limitations of drying thyme using the infrared-reflectance window method include the setup of the IR-RW dryer at a laboratory scale, controlled drying conditions, and specific ranges of process variables. In addition, future research directions could include validation of large-scale and pilot scale IR-RW drying systems; integration of renewable or hybrid energy sources to improve sustainability; and investigation of advanced hybrid drying approaches (e.g., infrared-ultrasound combinations) to enhance drying kinetics and preserve bioactive compounds.

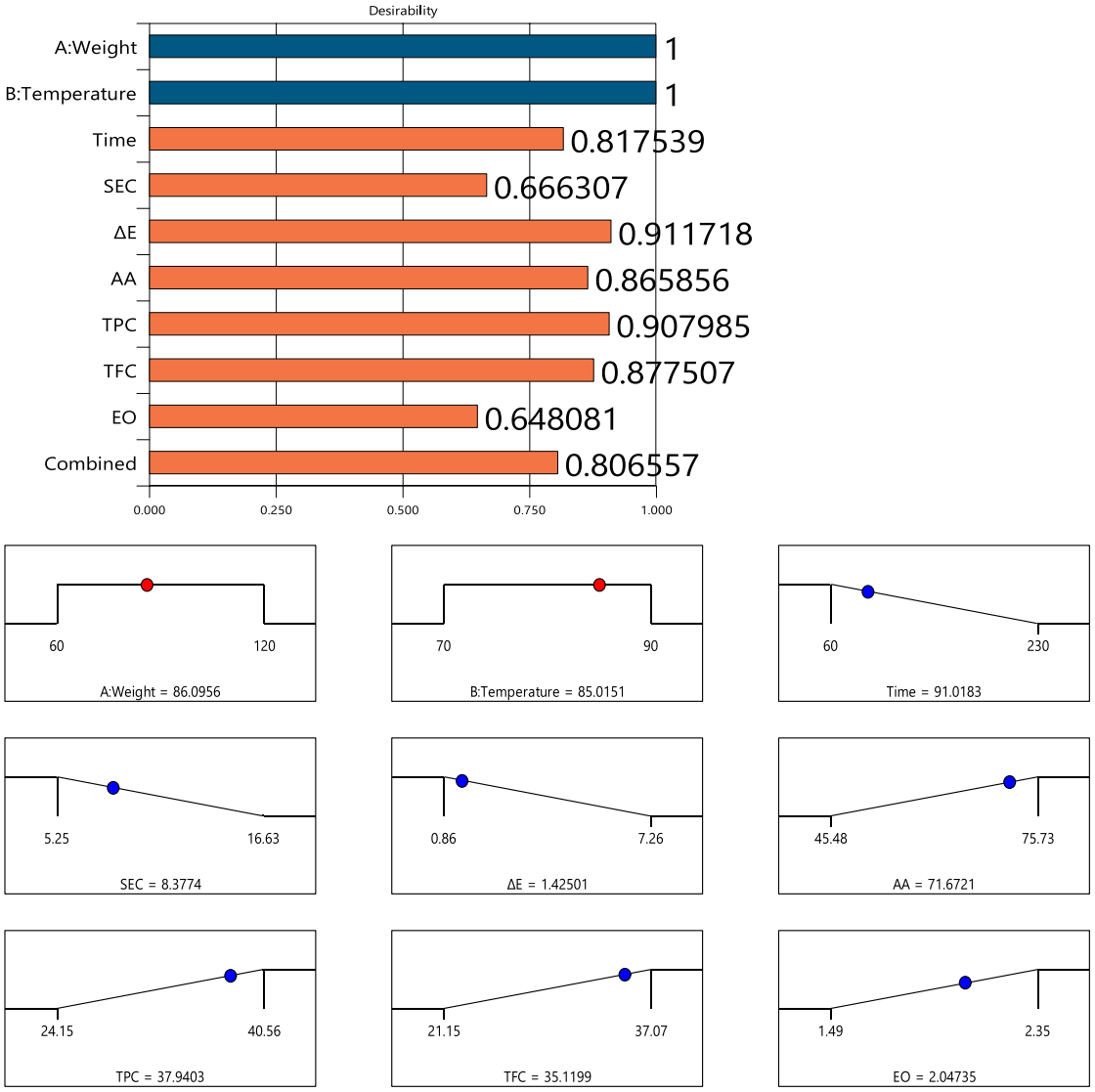

Fig. 7. Results for individual desirability values

Weight (g)	Temperature (°C)	Time	SEC	ΔE	AA	TPC	TFC	EO	Desirability	
86.103	85.02	91.003	8.37	1.42	71.68	37.93	35.11	2.04	0.807	

Table 12. Optimization results of thyme drying in the infrared- refractance window

Data availability

All data and materials are available upon reasonable request from the corresponding author.

Received: 10 January 2025; Accepted: 3 December 2025
Published online: 14 January 2026

References

1. Norouzi, Y., Ghobadi, M., Saeidi, M. & Dogan, H. Effect of nitrogen and cytokinin on quantitative and qualitative yield of thyme (*Thymus vulgaris* L.). *Agrotechn. Ind. Crops* **1**(1), 52–60 (2021).
2. Karami, H., Lorestani, A. N. & Tahvilian, R. Assessment of kinetics, effective moisture diffusivity, specific energy consumption, and percentage of thyme oil extracted in a hybrid solar-electric dryer. *J. Food Process Eng.* **44**(1), e13588 (2021).
3. Yilmaz, A., Alibas, I. & Asik, B. B. The effect of drying methods on the color, chlorophyll, total phenolic, flavonoids, and macro and micronutrients of thyme plant. *J. Food Process. Preserv.* **45**(11), e15915 (2021).
4. Wang, B., Wang, S. & Ling, B. Recent advances in the drying of medicinal herb by novel physical field-based techniques: a review. *J. Stored Prod. Res.* **112**, 102658 (2025).

5. Venkateshwari, T. et al. Thin-layer mathematical modeling for drying of turmeric slices in infrared dryer. *J. Food Process Eng.* **47**(4), e14601 (2024).
6. Muyonga, J. H. et al. Drying behaviour and optimization of drying conditions of pineapple puree and slices using refractance window drying technology. *J. Food Sci. Technol.* **59**, 2794–2803 (2022).
7. Khallaf, A. E. M. & El-Sebaii, A. Review on drying of the medicinal plants (herbs) using solar energy applications. *Heat Mass Transf.* **58**(8), 1411–1428 (2022).
8. Kaur, P., Zalpouri, R., Singh, M. & Verma, S. Process optimization for dehydration of shelled peas by osmosis and three-stage convective drying for enhanced quality. *J. Food Process. Preserv.* **44**, e14983 (2020).
9. Hii, C. L. et al. Hybrid drying of food and bioproducts: a review. *Drying Technol.* **39**, 1554–1576 (2021).
10. Waghmare, R. Refractance window drying: a cohort review on quality characteristics. *Trends Food Sci. Technol.* **110**, 652–662 (2021).
11. Zalpouri, R., Singh, M., Kaur, P. & Singh, S. Refractance window drying–a revisit on energy consumption and quality of dried bio-origin products. *Food Eng. Rev.* **14**(2), 257–270 (2022).
12. Seyfi, A., Asl, A. R. & Motevali, A. Comparison of the energy and pollution parameters in solar refractance window (photovoltaic-thermal), conventional refractance window, and hot air dryer. *Solar Energy* **229**, 162–173 (2021).
13. Acar, C., Dincer, I. & Mujumdar, A. A comprehensive review of recent advances in renewable-based drying technologies for a sustainable future. *Drying Technol.* **40**(6), 1029–1050 (2022).
14. Kaveh, M. et al. Review of advanced drying techniques: a path to lower greenhouse gas emissions in agriculture. *Discov. Sustain.* **6**(1), 423 (2025).
15. Rajoriya, D., Bhavya, M. L. & Hebbar, H. U. Far infrared assisted refractance window drying: influence on drying characteristics and quality of banana leather. *Drying Technol.* **7**, 1–3 (2023).
16. Sakare, P. et al. Infrared drying of food materials: Recent advances. *Food Eng. Rev.* **12**(3), 381–398 (2020).
17. Bernaert, N. et al. Innovative refractance window drying technology to keep nutrient value during processing. *Trends Food Sci. Technol.* **84**, 22–24 (2018).
18. Zamani, S., Bakhshi, D., Sahraroo, A. & Ebadi, M. T. Improvement of phytochemical and quality characteristics of dracocephalum kotschyi by drying methods. *Food Sci. Nutr.* **11**(7), 4246–4262 (2023).
19. Topuz, F. C., Bakkalbaşı, E., Aldemir, A. & Javidipour, I. Drying kinetics and quality properties of Mellaki (Pyrus communis L.) pear slices dried in a novel vacuum-combined infrared oven. *J. Food Process. Preserv.* **46**(10), e16866 (2022).
20. Geng, Z. et al. Characteristics and multi-objective optimization of carrot dehydration in a hybrid infrared/hot air dryer. *LWT* **172**, 114229 (2022).
21. Adak, N., Heybeli, N. & Ertekin, C. Infrared drying of strawberry. *Food chem.* **219**, 109–16 (2017).
22. Aktaş, M., Khanlari, A., Amini, A. & Şevik, S. Performance analysis of heat pump and infrared–heat pump drying of grated carrot using energy-exergy methodology. *Energy Convers. Manage.* **132**, 327–338 (2017).
23. Wang, D. et al. Effects of microwave power control on enzyme activity, drying kinetics, and typical nutrients of pleurotus eryngii: exploring the blanching mechanism by microstructural and ultrastructural evaluation. *J. Food Compos. Anal.* **128**, 106037 (2024).
24. Boateng, I. D., Yang, X. M. & Li, Y. Y. Optimization of infrareddrying parameters for Ginkgo biloba L.= seed and evaluation of product quality and bioactivity. *Ind. Crops Prod.* **160**, 113108 (2021).
25. Ebadi, M. T., Azizi, M., Sefidkon, F. & Ahmadi, N. Influence of different drying methods on drying period, essential oil content, and composition of Lippia citriodora Kunth. *J. Appl. Res. Med. Aromat. Plants* **2**(4), 182–187 (2015).
26. Xu, H. et al. Changes in water status and microstructure reveal the mechanisms by which tempering affects drying characteristics and quality attributes of medicinal chrysanthemums. *Ind. Crops Prod.* **205**, 117463 (2023).
27. Durgawati, B. & P. & Sutar, P.P.,. Development of a novel non-water infrared refractance window drying method for Malabar spinach: Optimization of process parameters using drying kinetics, mass transfer, and powder characterization. *Drying Technology* **41**(10), 1620–1635 (2023).
28. Mahanti, N. K. et al. Refractance windowTM-drying vs. other drying methods and effect of different process parameters on quality of foods: a comprehensive review of trends and technological developments. *Futur. Foods* **3**, 724 (2021).
29. Santos, V. C. S., Souza, R. L. D., Figueiredo, R. T. & Alsina, O. L. S. D. A review on refractance window drying process of fruits and vegetables: its integration with renewable energies. *Braz. J. Food Technol.* **25**, e2021153 (2022).
30. Raghavi, L. M., Moses, J. A. & Anandharamakrishnan, C. Refractance window drying of foods: a review. *J. Food Eng.* **222**, 267–275 (2018).
31. Menon, A., Stojceska, V. & Tassou, S. A. A systematic review on the recent advances of the energy efficiency improvements in non-conventional food drying technologies. *Trends Food Sci. Technol.* **100**, 67–76 (2020).
32. Hernandez-Santos, B. et al. Evaluation of physical and chemical properties of carrots dried by refractance window drying. *Drying Technol.* **34**, 1414–1422 (2016).
33. Rajoriya, D., Bhavya, M. L. & Hebbar, H. U. Impact of process parameters on drying behaviour, mass transfer and quality profile of refractance window dried banana puree. *LWT* **145**, 111330 (2021).
34. Dadhaneeya, H. et al. Impact of different drying methods on the phenolic composition, in vitro antioxidant activity, and quality attributes of dragon fruit slices and pulp. *Foods* **12**(7), 1387 (2023).
35. Rajoriya, D., Shewale, S. R. & Hebbar, H. U. Refractance window drying of apple slices: mass transfer phenomena and quality parameters. *Food Bioprocess Technol.* **12**, 1646–1658 (2019).
36. Baeghbali, V., Niakousari, M., Ngadi, M. O. & Hadi Eskandari, M. Combined ultrasound and infrared assisted conductive hydro-drying of apple slices. *Drying Technol.* **37**(14), 1793–1805 (2019).
37. Subrahmanyam, K. et al. Effect of cold plasma pretreatment on drying kinetics and quality attributes of apple slices in Refractance window drying. *Innov. Food Sci. Emerg. Technol.* **92**, 103594 (2024).
38. da Silva Simao, R. et al. Production of mango leathers by cast-tape drying: product characteristics and sensory evaluation. *LWT.* **99**, 445–452 (2019).
39. Zhang, Q. et al. Modified refractance window drying of jamun pulp (Syzygium cumini) based on innovative infrared and microwave radiation techniques. *Drying Technol.* **42**(5), 775–794 (2024).
40. Dadhaneeya, H. et al. The impact of refractance window drying on the physicochemical properties and bioactive compounds of malbhog banana slice and pulp. *Appl. Food Res.* **3**, 100279 (2023).
41. Simsek, M. & Süfer, Ö. Effect of pretreatments on refractance window drying, color kinetics and bioactive properties of white sweet cherries (Prunus avium L. stark gold). *J. Food Process. Preserv.* **45**(11), 5895. (2024).
42. Baeghbali, V., Niakousari, M. & Farahnaky, A. Refractance window drying of pomegranate juice: quality retention and energy efficiency. *LWT-Food Sci. Technol.* **66**(34), 40 (2016).
43. Tontul, I. & Topuz, A. Effects of different drying methods on the physicochemical properties of pomegranate leather (Pestil). *LWT.* **80**, 294–303 (2017).
44. Puente, L. et al. Refractance Window drying of goldenberry (Physalis peruviana L.) pulp: A comparison of quality characteristics with respect to other drying techniques. *LWT* **131**, 109772 (2020).
45. Zalpouri, R. et al. Drying kinetics, physicochemical and thermal analysis of onion puree dried using a refractance window dryer. *Processes* **11**(3), 700 (2023).

46. Rezvani, Z., Mortezapour, H., Ameri, M., Akhavan, H, & Arslan, S. Optimization of tomato slices drying in a continuous infrared-assisted refractance window™ dryer using response surface methodology. *Iranian Journal of Chemistry and Chemical Engineering*. 41 (12) (2022).
47. Uribe, E. et al. Assessment of refractive window drying of physalis (Physalis peruviana L.) puree at different temperatures: drying kinetic prediction and retention of bioactive components. *J. Food Meas. Charact.* **16**(4), 2605–2615 (2024).
48. Nguyen, T. V. L., Nguyen, Q. D. & Nguyen, P. B. D. Drying kinetics and changes of total phenolic content, antioxidant activity and color parameters of mango and avocado pulp in refractance window drying. *Polish J. Food Nutr. Sci.* **72**(1), 27–38 (2022).
49. Mandale, N. M., Attkan, A. K., Kumar, S. & Kumar, N. Drying kinetics and quality assessment of refractance window dried beetroot. *J. Food Process Eng.* **46**(7), e14332 (2023).
50. Zalpouri, R. et al. Mathematical and artificial neural network modelling for refractance window drying kinetics of coriander (Coriandrum sativum L.) followed by the determination of energy consumption, mass transfer parameters and quality. *Biomass Convers. Biorefinery* **15**, 967–983 (2025).
51. Kaveh, M., Zomorodi, S., Mariusz, S. & Dziwulska-Hunek, A. Determination of drying characteristics and physicochemical properties of mint (Mentha spicata L.) leaves dried in refractance window. *Foods* **13**(18), 2867 (2024).
52. Rajoriya, D., Shewale, S. R., Bhavya, M. L. & Hebbar, H. U. Far infrared assisted refractance window drying of apple slices: comparative study on flavour, nutrient retention and drying characteristics. *Innov. Food Sci Emerg. Technol.* **66**, 102530 (2020).
53. Baeghbali, V., Ngadi, M. & Niakousari, M. Effects of ultrasound and infrared assisted conductive hydro-drying, freeze-drying and oven drying on physicochemical properties of okra slices. *Innov. Food Sci. Emerg. Technol.* **63**, 102313 (2020).
54. Balasubramanian, P., Xiao, H. W. & Sutar, P. P. Effect of cyclic vacuum-steam blanching on the quality characteristics and functional properties of Malabar spinach (Basella alba) dried by non-water infrared refractance window drying. *Food Chem.* **465**, 141901 (2025).
55. AOAC. Official methods of analysis of AOAC International. 16th ed (Association of Official Analytical Chemist International AOAC, Gaithersburg, USA) 1997
56. Kaveh, M. et al. Energy and exergy analysis of drying terebinth in a far infrared-rotary dryer using response surface methodology. *Heat Transf.* **53**(8), 4109–4134 (2024).
57. Kaur, M., Bhatia, S., Kalsi, B. S. & Phutela, U. G. Unveiling the biomass conversion potential: study on drying methods' influence on polyphenols and linked antioxidant activities in euryhaline microalgal biomass with AI-predicted drying kinetics. *Biomass Conver. Biorefinery* https://doi.org/10.1007/s13399-024-05533-1 (2024).
58. Leilayi, M. et al. Energy and exergy efficiencies of batch paddy rice drying with liquefied petroleum gas dehumidification: a comprehensive analysis using adaptive neuro-fuzzy inference system and artificial neural networks approaches. *Energy Convers. Manage.: X* **25**, 100826 (2025).
59. Kalsi, B. S., Singh, S., Alam, M. S. & Bhatia, S. Microwave drying modelling of Stevia rebaudiana leaves using artificial neural network and its effect on color and biochemical attributes. *J. Food Qual.* **1**, 2811491 (2023).
60. Öztekin, Y. B. et al. Drying kinetics and thermodynamic properties of Uzun pistachios dried by convective drying. *J. Food Process. Preserv.* **46**(11), e17035 (2024).
61. Cunha, N., da Silva, L. H. M. & da Cruz Rodrigues, A. M. Drying of Curcuma longa L. slices by refractance window: Effect of temperature on thermodynamic properties and mass transfer parameters. *Heat Mass Transf.* **60**, 617–626 (2024).
62. Kaveh, M. et al. Machine learning approaches for estimating apricot drying characteristics in various advanced and conventional dryers. *J. Food Process Eng.* **46**(12), e14475 (2023).
63. Kırmızıkaya, E. S. & Doğan, I. Effect of different drying systems on drying performance of maraş green pepper (C. annum). *Turkish J. Agric.-Food Sci.Technol.* **11**(8), 1409–1414 (2023).
64. Santos, S. D. J. L., Silva, L. H. M. D. & Rodrigues, A. M. D. C. Prediction of mass transfer parameters and thermodynamic properties using the refractance Window TM technique for drying of Yam (Dioscorea Trifida) paste. *Food Sci. Technol.* **42**, e67021 (2022).
65. Sarpong, F. et al. Modeling of drying and ameliorative effects of relative humidity (RH) against β-carotene degradation and color of carrot (Daucus carota var.) slices. *Food Sci. Biotechnol.* **28**(1), 75–85 (2019).
66. Silva, N. C. B. et al. Drying kinetics and thermodynamic properties of boldo leaves (*Plectranthus barbatus* Andrews). *Cientifica* **47**(1), 1–7 (2019).
67. Motevali, A. & Koloor, R. T. A comparison between pollutants and greenhouse gas emissions from operation of different dryers based on energy consumption of power plants. *J. Clean. Prod.* **154**, 445–461 (2017).
68. Kaveh, M. et al. Comparative evaluation of greenhouse gas emissions and specific energy consumption of different drying techniques in pear slices. *Euro. Food Res. Technol.* **249**(12), 3027–3041 (2023).
69. Bardakçi, M. S. & Karacabey, E. Drying of tarhana dough by refractance window™ technology under vacuum/atmospheric conditions: characterization of physical and quality parameters. *Food Sci. Nutr.* **12**(2), 971–984 (2024).
70. Rostami Gharkhloo, Z., Sharifian, F., Rahimi, A. & Akhoundzadeh Yamchi, A. Influence of high wave sound pretreatment on drying quality parameters of Echinacea root with infrared drying. *J. Sci. Food Agric.* **102**(5), 2153–2164 (2022).
71. Kalsi, B. S., Singh, S., Alam, M. S. & Sidhu, G. K. Comparison of ANN and ANFIS modeling for predicting drying kinetics of Stevia rebaudiana leaves in a hot-air dryer and characterization of dried powder. *Int. J. Food Prop.* **26**(2), 3356–3375 (2023).
72. Rekik, C. et al. Energy saving and quality preservation through modulating time related conditions during interval drying of pumpkin (Cucurbita maxima). *Food. Bioprod. Process.* **144**, 220–233 (2024).
73. Beigi, M. Thin layer drying of wormwood (Artemisia absinthium L.) leaves: dehydration characteristics, rehydration capacity and energy consumption. *Heat Mass Transf.* **53**(8), 2711–2718 (2017).
74. Meshkat, H. et al. Analysis of energy and exergy of lavender extract powder in spray dryer. *Heat Transf.* **43**(8), 4608–4624 (2024).
75. Bala, M. et al. An innovative approach to biomass utilization through concurrent hesperidin and pectin extraction from immature dropped kinnow (Citrus reticulata) fruits. *J. Food Meas. Charact.* **18**(9), 7953–7966 (2024).
76. Kumar, M., Madhumita, M., Srivastava, B. & Prabhakar, P. K. Mathematical modeling and simulation of refractance window drying of mango pulp for moisture, temperature, and heat flux distribution. *J. Food Process Eng.* **45**(9), e14090 (2022).
77. Pal, L. et al. Mass transfer parameters and quality characteristics of aonla slices under refractance window drying. *Drying Technol.* **42**(3), 492–505 (2024).
78. Adekanye, T., Okunola, A., Moses, O., Idahosa, E., Boye, Y. & Saleh, A. Mathematical modelling of drying parameters of Moringa oleifera leaves in a cabinet dryer. *Research in Agricultural Engineering* 69 (4) (2023)
79. Nurmawati, T., Hadiyanto, H., Cahyadi, C., Fachrizal, N. Sutopo, S. Efficiency and energy consumption analysis of infrared-assisted drying of oyster mushrooms. *International Journal of Heat & Technology 41* (4) (2023)
80. Ayala-Aponte, A. A., Cárdenas-Nieto, J. D. & Tirado, D. F. Aloe vera gel drying by Refractance Window®: Drying kinetics and high-quality retention. *Foods* **10**(7), 1445 (2021).
81. Akhoundzadeh Yamchi, A. A., Sharifian, F., Khalife, E. & Kaveh, M. Drying kinetic, thermodynamic and quality analyses of infrared drying of truffle slices. *J. Food Sci.* **89**(6), 3666–3686 (2024).
82. Turan, O.Y. & Firatligil, F.E. Modelling and characteristics of thin layer convective air-drying of thyme (Thymus vulgaris) leaves. *Czech Journal of Food Sciences 37* (2) (2019)
83. de Vilela Silva, E. T. et al. Enhancing mangosteen peel drying: Impact of ethanol pre-treatment, vacuum pulsing, and blanching on process efficiency and bioactive compound levels. *LWT* **198**, 115981 (2024).

84. Moura, R. L. et al. Smelling peppers and pout submitted to convective drying: mathematical modeling thermodynamic properties and proximal composition. *Foods* **12**(11), 2106 (2023).
85. Rashid, M. T. et al. Drying kinetics and quality dynamics of ultrasound-assisted dried selenium-enriched germinated black rice. *Ultrason. Sonochem.* **98**, 106468 (2023).
86. Santos, N. C. et al. Effect of pulse electric field (PEF) intensity combined with drying temperature on mass transfer, functional properties, and in vitro digestibility of dehydrated mango peels. *J. Food Meas. Charact.* **17**(5), 5219–5233 (2023).
87. Yıldırım, A. Influence of temperature, ultrasound, and variety on moisture diffusivity and thermodynamic properties of some durum wheat varieties during hydration. *J. Food Process. Preserv.* **46**(4), e16463 (2022).
88. Reis, C. G. D. et al. Pineapple peel flours: drying kinetics, thermodynamic properties, and physicochemical characterization. *Processes* **11**(11), 3161 (2023).
89. Santos, N. C. et al. Effect of ultrasound pre-treatment on the kinetics and thermodynamic properties of guava slices drying process. *Innov. Food Sci. Emerg. Technol.* **66**, 102507 (2020).
90. Selvakumarasamy, S., Rengaraju, B., Kulathooran, R. & Tarafdar, A. Artificial neural network and mathematical modeling on the drying kinetics of Costus pictus rhizomes and its impact on the polyphenol, flavonoid content and antioxidant activity. *Biomass Convers. Biorefinery* **15**, 2537 (2023).
91. Wang, Z. et al. Effect of boiling on water mobility, quality and structure characteristics of Mactra veneriformis during hot air drying. *LWT* **179**, 114690 (2023).
92. Rodríguez-Ramos, F. et al. Mathematical modeling and quality parameters of Salicornia fruticosa dried by convective drying. *J. Food Sci. Technol.* **58**, 474–483 (2021).
93. Kaveh, M. et al. Impact of various drying technologies for evaluation of drying kinetics, energy consumption, physical and bioactive properties of Rose flower. *Sci. Rep.* **15**, 9245 (2025).
94. Vega-Galvez, A. et al. Convective hot air drying of red cabbage (Brassica oleracea var. Capitata Rubra): mathematical modeling, energy consumption and microstructure. *Processes* **12**(3), 509 (2024).
95. Fabani, M. P., Román, M. C., Rodriguez, R. & Mazza, G. Minimization of the adverse environmental effects of discarded onions by avoiding disposal through dehydration and food-use. *J. Environ. Manage.* **271**, 110947 (2020).
96. Doymaz, I. Drying of thyme (Thymus vulgaris L.) and selection of a suitable thin-layer drying model. *J. Food Process. Preserv.* **35**(4), 458–465 (2011).
97. Kaveh, M. et al. Effect of ethanol and ultrasonic pretreatments on drying kinetics, quality, and physicochemical attributes of dried Salvia officinalis. *Biomass Convers. Biorefinery* https://doi.org/10.1007/s13399-025-06916-8 (2025).
98. Golla, S. P. et al. Meta analysis on color, total flavonoids, antioxidants, frictional, mechanical, and cutting force of moringa pods. *J. Food Process Eng.* **45**(10), e14136 (2022).
99. Hassan, A. M. & Koca, I. Evaluation of physicochemical characteristics, bioactive properties, drying kinetics, and rehydration of convective dried autumn olive berries as a source of functional food ingredients. *J. Food Meas. Charact.* **16**(6), 4947–4975 (2022).
100. Tuteja, S., Mondal, I. H. & Dash, K. K. Conductive hydro drying of ripened papaya: optimization and product characterization. *Food Sci. Biotechnol.* **33**, 2571 (2024).
101. Padhi, S., Murakonda, S. & Dwivedi, M. Investigation of drying characteristics and nutritional retention of unripe green banana flour by refractance window drying technology using statistical approach. *J. Food Meas. Charact.* **16**(3), 2375–2385 (2022).
102. Setareh, R., Mohammadi-Ghermezgoli, K., Ghaffari-Setoubadi, H. & Alizadeh-Salteh, S. The effectiveness of hot-air, infrared and hybrid drying techniques for lemongrass: appearance acceptability, essential oil yield, and volatile compound preservation. *Sci. Rep.* **13**(1), 18820 (2023).

Author contributions

MK. and S.Z: Investigation, supervision, Conceptualization, Methodology, data curation, Software, data analysis and writing—original draft preparation., M.H.R., M.S. and A.D.H.: Methodology, validation, Investigation, resources, writing—review & editing, and investigation All authors have read and agreed to the published version of the manuscript.

Funding

The authors would like to thank Iran National Scientific Foundation (INSF) for the financial support of project no 4020272.

Declarations

Competing interests

I declare that the authors have no competing interests as defined by Nature Research, or other interests that might be perceived to influence the results and/or discussion reported in this paper.

Additional information

Correspondence and requests for materials should be addressed to S.Z. or S.M.